

Spectrum Management and Power Allocation in ¹ MIMO Cognitive Networks

Diep N. Nguyen and Marwan Krunz

Department of Electrical and Computer Engineering, University of Arizona

E-mail: {dnnguyen, krunz}@ece.arizona.edu

Technical Report

TR-UA-ECE-2011-2

Last Updated: January 16, 2012

Abstract

Cognitive radio (CR) techniques improve the spectrum utilization by exploiting temporarily-free frequency bands (i.e., in the time domain). The spectrum utilization can be boosted further if CR nodes are equipped with multiple antennas to leverage communications in the spatial dimension. In this article, we consider the problem of maximizing the throughput of a multi-input multi-output (MIMO) cognitive radio network. With spatial multiplexing performed over each frequency band, a multi-antenna CR node controls its antenna radiation pattern and allocates power for each data stream by appropriately adjusting its *precoding matrix*. Our objective is to design a set of precoding matrices (one for each band) at each CR node so that power and spectrum are optimally allocated for that node (in terms of throughput) and its interference is steered away from other CR and PR transmissions. In other words, the problems of power, spectrum allocation and interference management are jointly investigated. We come up with a multi-carrier MIMO network throughput optimization problem subject to frequency-dependent power constraints. The problem is non-convex, with the number of variables growing quadratically with the number of antenna elements. To tackle it, we translate it into a noncooperative game. We then derive an optimal pricing policy for each node, which adapts to the node's neighboring conditions and drives the game to a Nash-Equilibrium (NE). The network throughput under

this NE is equal to that of a locally optimal solution of the non-convex centralized problem. To find the set of precoding matrices at each node (best response), a low-complexity distributed algorithm is developed by exploiting the strong duality of the per-user convex optimization problem. The number of variables in the distributed algorithm is independent to the number of antenna elements. A centralized (cooperative) algorithm is also developed, serving as a performance benchmark. Simulations show that the network throughput under the distributed algorithm converges rapidly to that of the centralized one. We then develop a MAC protocol that implements our resource allocation and beamforming scheme. Extensive simulations show that the proposed protocol dramatically improves the network throughput as well as reduces the power consumption. The application of our results is not limited to CR systems, but extends to any multi-carrier (e.g., OFDM) MIMO system.

Index Terms

Noncooperative game, pricing, cognitive radio, MIMO, MAC protocol, power allocation, frequency management, beamforming.

I. INTRODUCTION

Recent years have witnessed great research interests in cognitive radio (CR) and multi-input multi-output (MIMO) systems. While the former is viewed as a key enabling technology to improve spectrum utilization, the later has already proved itself as a powerful signal processing technique to improve spectral efficiency. Through sensing and/or probing, CRs can opportunistically communicate on temporarily available spectrum bands while avoiding interference with licensed-spectrum (or primary radio-PR) users. MIMO communications improve the channel capacity by sending independent data streams simultaneously over different antennas (a technique known as *spatial multiplexing*).

A crucial challenge in CR research is how to effectively allocate transmission powers and spectrum among CRs (see Figure 2(a)) so as to maximize network throughput while avoiding interfering with PR receptions. Even for a single frequency band and single-antenna wireless devices, the problem is difficult due to the non-convexity of the network throughput function. For single-antenna CRs, distributed algorithms were developed in [1] [2] using game theory.

The incorporation of MIMO techniques into CR systems introduces two new control dimensions (besides

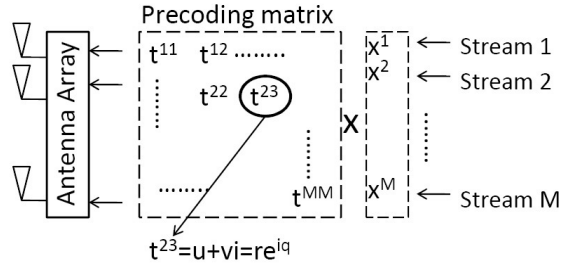


Fig. 1. MIMO precoding method.

power control and frequency management): power allocation over antennas (space dimension) and interference management. The latter comes from MIMO's *degrees of freedom* [3], which allow a MIMO node to suppress interference from others (by using some of its antennas) and configure its antenna radiation patterns to keep interference away from unintended receivers. MIMO's power allocation and interference management can be jointly controlled via *precoding matrices*, a spatial multiplexing technique [3] (Figure 1). Using this technique, the vector of information symbols are pre-multiplied with a matrix before being placed on a transmit antenna array. By tuning the amplitude and the phase of each complex entry in the precoding matrix, one adjusts not only the allocated powers but also the radiation directions, which together shape the antenna radiation patterns. Previous MIMO-networking works [4] [5] [6] considered power allocation or *stream control* (Figure 2(b)) but did not take into account interference management via controlling antenna beams. An optimal set of precoding matrices for each node would be one that allocates power over *both* space and frequency dimensions (2(c)) *and* yields radiation patterns that induce minimum interference (2(d)), so as to maximize the network throughput. This problem is the focus of our work.

II. RELATED WORKS

If one ignores the need to protect PR receptions, a MIMO-based CR system very much resembles a multi-carrier (e.g., OFDM) MIMO (MC-MIMO) system. In MC-MIMO, joint power and spectrum optimization is a non-convex problem, which is attributed to co-channel multi-user interference. Globally optimal solvers for non-convex problems, e.g., branch and bound, often have exponentially growing complexity in the number of variables. Unfortunately, the number of variables in a MC-MIMO network can be very large. For instance, when using the precoding technique with 4 antennas per node and 10 sub-carriers in a network of 10 links,

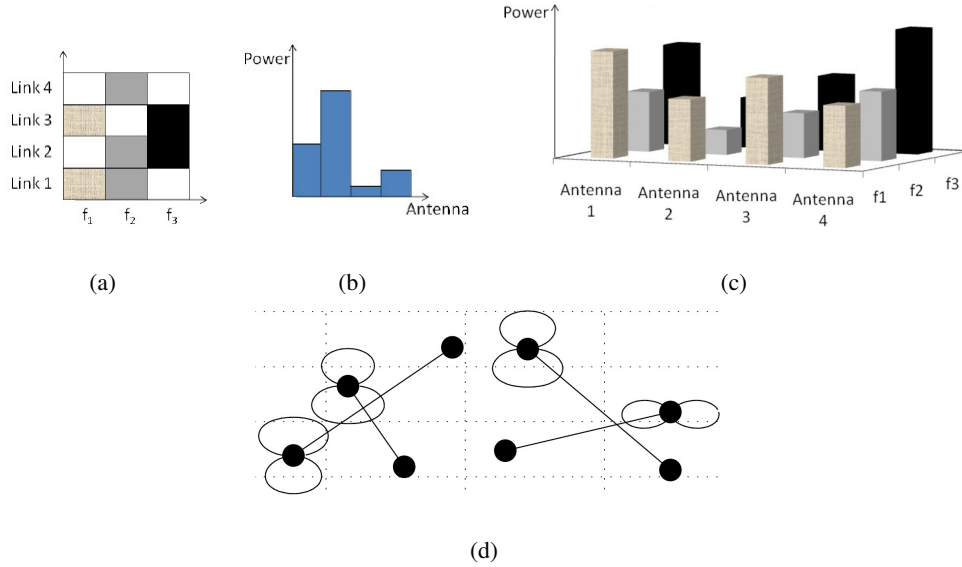


Fig. 2. Power allocation in either frequency (a) or space dimension (b) or in both dimensions (c) and four transmit radiation patterns steering away from nearby receivers (d).

this number is $4 \times 4 \times 10 \times 10 = 1600$ complex variables (or 3200 real variables). The latest advances in power and spectrum management for MC-MIMO can be found in [7] using dual stochastic optimization. Similar to the aforementioned works, the authors in [7] [8] only considered the power allocation (the amplitude) but did not optimize the antenna radiation directions (the phase).

In addition to imposing constraints to protect PRs, we consider a full/generalized eigen precoding MIMO CR network. In the literature, there have been a vast body of works on MIMO precoding-matrix design, categorized into beamforming and generalized eigencoding. In beamforming (e.g., [9] [10] for MIMO networks and [11] for MIMO CRNs), there is only one data stream to be sent, hence all precoding matrices reduce to vectors (matrices of rank one). In generalized eigencoding, there is no constraint on the rank of the precoding matrices [12], i.e., several data streams can be sent simultaneously. Inspired by the introduction of the spatial multiplexing technique into existing networks (e.g., 802.11n allows up to four concurrent multiplexed streams), generalized eigencoding has recently attracted great interests.

There have been recent works at the physical layer that attempt to protect PR communications in a MIMO CR network (CRN) while maximizing the CRN's throughput (e.g., [11] [13] [14]). These works assumed full or partial availability of channel state information (CSI) from each CR to each PR. This requires feedback or coordination between CRs and PRs. However, current licensed radio devices are not ready for

such a feedback mechanism, as CR communications are expected to be transparent to PRs. Authors in [15] provided a MIMO CR scheme which is robust to CR-PR CSI estimation error by dealing with the worst case error. In our setup, PR communications are protected by imposing frequency-dependent constraint on the transmission power of CRs. This assumption has been used in single-antenna CRNs e.g., [2] [16]. Our work is in line with the joint resource allocation and waveform adaptation developed in [16] for single antenna CRNs and without a pricing policy. Though we limit our analysis to the case of using power masks to focus on the beamforming and spectrum sharing among MIMO CR nodes, it should be noted that the formulation and analysis here are also applicable to CR systems that adapt the CR transmission parameters to the surrounding environment [17] as well as the error-robust scheme in [15].

Because of the challenges associated with power and spectrum optimization, most existing works on MIMO CR systems (e.g., [18] [15] [14]) do not consider optimization over the frequency dimension. The extension of these works to multi-band MIMO CRNs is not trivial. First, scalar-value algorithms (e.g., the bisection search in [14]) used for a single-band MIMO ad hoc network will not work when searching for optimal vectors in multi-band MIMO CRNs. Second, we show that even without beamforming, the optimal power allocation over both frequency and spatial dimensions is not equivalent to a general water filling problem [19](with multiple water levels), then cannot be treated using existing algorithms [20] [19] [21]. Third, if one separately applies results from single-band MIMO to each individual band of a multi-band MIMO CR system, the achieved throughput is often low, as the resulting network operation points do not meet the optimal conditions (discussed later). In this paper, simulations are used to compare the performance of such approaches to that of our algorithms. Additionally, it should be noted that the MIMO CR game-based analysis in [18] [15] did not use a pricing mechanism. Simulations showed that our pricing technique greatly outperforms non-pricing-based mechanisms in terms of both network throughput and power efficiency.

Motivated by the above, the objective of this paper is to develop low-complexity distributed algorithms that configure the transmit antenna radiation directions and allocate power over all data streams, specified by space (subindex s) and frequency (subindex k) dimensions, so that the MIMO CRN's throughput is maximized. We model this joint problem of power, spectrum allocation and beamforming as a price-based

noncooperative game [22]. To manage interference, we derive a diagonal block pricing-factor matrix. This matrix is user-dependent, and is used to capture the interference effect from a transmitter to unintended receivers. Hence, it is a function of the node's precoding matrices as well as its neighboring receivers. The pricing-factor matrix does not only improve the Nash-Equilibrium (NE) of the game, but also drives the game towards a locally optimal point of the centralized problem. Exploiting the strong duality in convex optimization, we design a low-complexity distributed algorithm to determine the set of precoding matrices (*best response*) for each node. The dimensionality of the distributed algorithm is only $K + 1$, where K is the number of frequency bands, i.e., it does not depend on the antenna array size. We also develop a centralized algorithm for the network optimization problem, where nodes are assumed to work in a cooperative way (cooperative game). Simulations results show that the performance of the distributed algorithm is almost the same as that of the centralized one.

Throughout the paper, we use $(\cdot)^*$ to denote the conjugate matrix, $(\cdot)^H$ to denote the Hermitian matrix transpose, $\text{tr}(\cdot)$ for the trace of a matrix, $\det(\cdot)$ for the determinant, and $(\cdot)^T$ for matrix transpose. Matrices and vectors are indicated in boldface.

In Section III, we present the network model and the problem formulation. The noncooperative game analysis, optimal pricing policy, convergence proof, the distributed algorithm and a corresponding MAC protocol are given in Section IV. The centralized algorithm is developed using augmented Lagrangian multipliers in Section V. Numerical results are discussed in Section VI. Concluding remarks are provided in Section VII.

III. PROBLEM FORMULATION

We consider a CRN that coexists with several PR networks. The CRN consists of N links. Each CR node is equipped with M antennas. The spectrum to be allocated is comprised of K orthogonal frequency bands (referred to as channels) that have central frequencies f_1, f_2, \dots, f_K . Let $\Phi_N \stackrel{\text{def}}{=} \{1, 2, \dots, N\}$ and $\Psi_K \stackrel{\text{def}}{=} \{1, 2, \dots, K\}$ denote the sets of CR links and channels, respectively. Each CR user i can simultaneously communicate over multiple frequency bands, denoted by the set S_i . We impose a half-

duplex constraint on all transmissions, meaning that a CR cannot transmit and receive at the same time.

The transmitter of each CR link can send up to M independent data streams on its M antennas over a given channel. A node controls the emitted antenna pattern and power allocation for these streams through its precoding matrices. Formally, for frequency band f_k , let $\mathbf{x}_i^{(k)}$ be a column vector of M information symbols, sent from node i to its destination node $d(i)$. Each element of $\mathbf{x}_i^{(k)}$ belongs to one data stream. Let $\tilde{\mathbf{T}}_i^{(k)}$ denote the precoding matrix of node i on frequency band f_k . Then, the actual transmit vector is $\tilde{\mathbf{T}}_i^{(k)} \mathbf{x}_i^{(k)}$.

We allow for spectrum sharing among different CR links. This assumption is in contrast to the case that restricts to one CR transmission on a given frequency channel in the same neighborhood. In our setup, several CR links can simultaneously occupy the same channel. Specifically, for a frequency band f_k , the received signal vector $\mathbf{y}_{d(i)}^{(k)}$ at the receiver $d(i)$ of link $(i, d(i))$ is given by:

$$\mathbf{y}_{d(i)}^{(k)} = \mathbf{H}_{d(i),i}^{(k)} \tilde{\mathbf{T}}_i^{(k)} \mathbf{x}_i^{(k)} + \sum_{j \in \Phi_N \setminus \{i\}} \mathbf{H}_{d(i),j}^{(k)} \tilde{\mathbf{T}}_j^{(k)} \mathbf{x}_j^{(k)} + \mathbf{N}_k \quad (1)$$

where the first term in the RHS of (1) is the desired signal sent from transmitter i and $\mathbf{H}_{d(i),i}^{(k)}$ is the channel gain matrix on frequency band f_k from the transmitter i to the receiver $d(i)$. Specifically, $\mathbf{H}_{d(i),i}^{(k)} \stackrel{\text{def}}{=} |\mathbf{h}_1 \mathbf{h}_2 \dots \mathbf{h}_M|$, where \mathbf{h}_s is an $M \times 1$ column vector of channel gains from transmit antenna s to all M receiving antennas, $s = 1, \dots, M$. We assume a flat-fading channel. Each entry of $\mathbf{H}_{d(i),i}^{(k)}$ is a complex Gaussian variable with zero mean and unit variance. The second term in the expression of $\mathbf{y}_{d(i)}^{(k)}$ represents interference from other CR links that share channel f_k with link $(i, d(i))$. \mathbf{N}_k is an $M \times 1$ complex Gaussian noise vector with identity covariance matrix \mathbf{I} , representing the noise floor as well as normalized (and whiten) interference from nearby PR users on band k .

The Shannon capacity of link $(i, d(i))$, referred to as (i) for short, on the frequency band f_k is [3]:

$$R_{(i)}^{(k)} = \log \det(\mathbf{I} + \tilde{\mathbf{T}}_i^{(k)H} \mathbf{H}_{d(i),i}^{(k)H} \mathbf{C}_{d(i)}^{(k)-1} \mathbf{H}_{d(i),i}^{(k)} \tilde{\mathbf{T}}_i^{(k)}) \quad (2)$$

where $\mathbf{C}_{d(i)}^{(k)}$ is the noise-plus-interference covariance matrix at $d(i)$ over frequency band f_k , given by:

$$\mathbf{C}_{d(i)}^{(k)} = \mathbf{I} + \sum_{j \in \Phi_N \setminus \{i\}} \mathbf{H}_{d(i),j}^{(k)} \tilde{\mathbf{T}}_j^{(k)} \tilde{\mathbf{T}}_j^{(k)H} \mathbf{H}_{d(i),j}^{(k)H}.$$

The total channel rate over all frequency bands of link i is:

$$R_{(i)} = \sum_{k \in \Psi_K} R_{(i)}^{(k)}. \quad (3)$$

We use $P_{s,k}^{(i)}$ to denote the power allocated on band k (frequency dimension) at stream s (space dimension or antenna) of CR user i . $P_{s,k}^{(i)}$ is the entry (s, s) on the diagonal of matrix $(\tilde{\mathbf{T}}_i^{(k)} \tilde{\mathbf{T}}_i^{(k)H})$. For user i , the total power allocated on all frequency bands and all antennas should not exceed its maximum power budget P_{\max} (we assume an identical power limit for all CR users). Consequently,

$$\sum_{k \in \Psi_K} \sum_{s=1}^M P_{s,k}^{(i)} = \sum_{k \in \Psi_K} \text{tr}(\tilde{\mathbf{T}}_i^{(k)} \tilde{\mathbf{T}}_i^{(k)H}) \leq P_{\max}. \quad (4)$$

Spectrum sharing between CR and PR transmissions takes two forms: *spectrum overlay* and *spectrum underlay*. In the former, CRs only occupy a channel if on that channel, no PR is detected (also known as a *detect-and-avoid* mechanism). Spectrum underlay allows CR users to occupy a channel even if PRs are detected, provided that the transmissions of CRs do not deteriorate the quality of service for the PR users. There are two methods to realize underlay spectrum sharing: *static* and *dynamic*. The static method requires that the transmit power of CRs on frequency channel f_k is always less than a given power mask $P_{\text{mask}}(f_k)$. Let $\mathbf{P}_{\text{mask}} \stackrel{\text{def}}{=} (P_{\text{mask}}(f_1), P_{\text{mask}}(f_2), \dots, P_{\text{mask}}(f_K))$ denote the power mask on all channels. Instead of specifying hard constraints on the transmit powers of CRs, the dynamic method adapts these transmit powers to activities from neighboring PRs and other CRs so that the *accumulated* interference (from all CRs and PRs) at a nearby PR receiver does not exceed a threshold. Though the dynamic method may result in higher network throughput, it requires coordination among CRs and PRs and can only statistically guarantee the PRs' quality of service. This is due to the fact that it is impractical to perfectly model and

estimate the interference from CR and PR links. In this paper, we use the static method, implying that:

$$\sum_{s=1}^M P_{s,k}^{(i)} = \text{tr}(\tilde{\mathbf{T}}_i^{(k)} \tilde{\mathbf{T}}_i^{(k)H}) \leq P_{mask}(f_k). \quad (5)$$

It should be noted that the subsequent analysis is also applicable to the dynamic method and the detect-and-avoid mechanism.

We aim at maximizing the CRN throughput. Mathematically, the network optimization problem can be stated as follows:

$$\begin{aligned} & \underset{\{\tilde{\mathbf{T}}_i^{(k)}, \forall k \in \Psi_K, \forall i \in \Phi_N\}}{\text{maximize}} && \sum_{i \in \Phi_N} R_{(i)} \\ & \text{s.t.} && \\ & \text{C1:} && \sum_{k \in \Psi_K} \text{tr}(\tilde{\mathbf{T}}_i^{(k)} \tilde{\mathbf{T}}_i^{(k)H}) \leq P_{\max}, \quad \forall i \in \Phi_N \\ & \text{C2:} && \text{tr}(\tilde{\mathbf{T}}_i^{(k)} \tilde{\mathbf{T}}_i^{(k)H}) \leq P_{mask}(f_k), \quad \forall k \in \Psi_K, \forall i \in \Phi_N. \end{aligned} \quad (6)$$

IV. GAME THEORETIC DESIGN

The network optimization problem (6) is not convex due to the presence of interference among CR users that share the same frequency band. Thus, even in a centralized manner, computing the globally optimal solution is prohibitively expensive. Thus, we reformulate it using game theory and derive a pricing function for each CR link that guarantees a locally optimal solution for problem (6), found in a distributed manner.

A. Game Formulation

A noncooperative game is characterized by its set of players, their action/strategy space, and their utility/payoff functions. For the underlying CRN, the set of CR links Φ_N represents the set of players. The action space is the union of the action spaces of various players, subject to constraints C1 and C2 in (6). The action/strategy space for each player is the set of all possible precoding matrices for the K frequency channels in Ψ_K . Formally, an action from the action space of link i is denoted by $\tilde{\mathbf{T}}_i \stackrel{\text{def}}{=} (\tilde{\mathbf{T}}_i^{\{1\}}, \tilde{\mathbf{T}}_i^{\{2\}}, \dots, \tilde{\mathbf{T}}_i^{(k)})$, which can be viewed as an $M \times KM$ block matrix, comprised of K $M \times M$ matrices. Let $\tilde{\mathbf{T}}_{-i} \stackrel{\text{def}}{=} (\tilde{\mathbf{T}}_1, \tilde{\mathbf{T}}_2, \dots, \tilde{\mathbf{T}}_{i-1}, \tilde{\mathbf{T}}_{i+1}, \dots, \tilde{\mathbf{T}}_N)$ be the set of actions from all links, except link i .

The utility or payoff of player i for its action $\tilde{\mathbf{T}}_i$ is mapped to link i 's Shannon rate, which also depends on the selection of the precoding matrices from other CR links $\tilde{\mathbf{T}}_{-i}$:

$$\begin{aligned} U_i(\tilde{\mathbf{T}}_i, \tilde{\mathbf{T}}_{-i}) &\stackrel{\text{def}}{=} R_{(i)} \\ &= \sum_{k \in \Psi_K} \log \det(\mathbf{I} + \tilde{\mathbf{T}}_i^{(k)H} \mathbf{H}_{d(i),i}^{(k)H} \mathbf{C}_{d(i)}^{(k)-1} \mathbf{H}_{d(i),i}^{(k)} \tilde{\mathbf{T}}_i^{(k)}). \end{aligned} \quad (7)$$

Due to the noncooperative nature of the game, the transmitter of each link allocates its transmission power over both space and frequency dimensions, and configures its radiation directions to maximize its own return. Formally, each CR user i solves the following problem for its precoding matrix set $\tilde{\mathbf{T}}_i$:

$$\begin{aligned} &\underset{\{\tilde{\mathbf{T}}_i^{(k)}, \forall k \in \Psi_K\}}{\text{maximize}} && U_i(\tilde{\mathbf{T}}_i, \tilde{\mathbf{T}}_{-i}) \\ &\text{s.t.} && \\ &\text{C1}': && \sum_{k \in \Psi_K} \text{tr}(\tilde{\mathbf{T}}_i^{(k)} \tilde{\mathbf{T}}_i^{(k)H}) \leq P_{\max} \\ &\text{C2}': && \text{tr}(\tilde{\mathbf{T}}_i^{(k)} \tilde{\mathbf{T}}_i^{(k)H}) \leq P_{\text{mask}}(f_k), \quad \forall k \in \Psi_K. \end{aligned} \quad (8)$$

By solving the above problem, CR users implicitly interact with each other through their choice of the precoding matrices. Under some conditions, the game reaches a NE where no CR user has incentive to unilaterally deviate from. However, as each CR user behaves selfishly, the resulting NE is often far from the Pareto optimum, and network throughput can be low.

To drive the above noncooperative game to a better NE, i.e., achieve higher social welfare, we use a pricing or taxation mechanism to encourage selfish players to work in a cooperative manner [23]. Pricing makes players more socially responsible for their actions. The utility function with price is defined as follows:

$$U'_i(\tilde{\mathbf{T}}_i, \tilde{\mathbf{T}}_{-i}) \stackrel{\text{def}}{=} U_i(\tilde{\mathbf{T}}_i, \tilde{\mathbf{T}}_{-i}) - F_u(\tilde{\mathbf{T}}_i) \quad (9)$$

where $F_u(\tilde{\mathbf{T}}_i)$ is the pricing function for link i . Consequently, we come up with the following noncooperative

game with pricing:

$$\begin{aligned}
& \underset{\{\tilde{\mathbf{T}}_i^{(k)} \forall k \in \Psi_K\}}{\text{maximize}} && U'_i(\tilde{\mathbf{T}}_i, \tilde{\mathbf{T}}_{-i}), \quad \forall i \in \Phi_N \\
& \text{s.t.} && \\
& && \text{C1' and C2' as in problem (8).}
\end{aligned} \tag{10}$$

B. Pricing Policy

A Pareto-optimal pricing policy is one that drives the game to a NE on the Pareto frontier. An optimal pricing policy is one that yields the game to a NE that is identical to the globally optimal solution of the non-convex problem (6). However, deriving such a pricing function is often difficult for two reasons. First, it is hard to characterize the optimal or the Pareto-optimal pricing policy, making it not possible to quantify the performance gap between these policies and the achieved NE. Second, an optimal pricing function that requires global network information is impractical for a distributed network. To improve the efficiency of the NE, the pricing functions in the literature are usually based on heuristics. For instance, the pricing functions in [24] are suboptimal linear functions with a fixed pricing-factor.

In economics, the pricing function can take various forms to account for various marketing and pricing policies, e.g., volume discount, coupon discount, etc. In the context of network resource allocation, both linear (e.g., [2] [25]) and nonlinear [1] pricing functions have been proposed. In this paper, we define the pricing function $F_u(\tilde{\mathbf{T}}_i)$ as follows:

$$F_u(\tilde{\mathbf{T}}_i) = \text{tr} \left[\tilde{\mathbf{T}}_i^H \times \mathbf{A}_i \times \tilde{\mathbf{T}}_i \right] \tag{11}$$

where

$$\mathbf{A}_i = \begin{bmatrix} \mathbf{A}_i^{(1)} & \mathbf{0} & \cdots & \mathbf{0} \\ \mathbf{0} & \mathbf{A}_i^{(2)} & \cdots & \mathbf{0} \\ \vdots & \vdots & \ddots & \vdots \\ \mathbf{0} & \mathbf{0} & \cdots & \mathbf{A}_i^{(K)} \end{bmatrix} \tag{12}$$

is an $KM \times KM$ block diagonal matrix, consisting of K blocks along its diagonal. The k th block $\mathbf{A}_i^{(k)}$ is

an $M \times M$ positive-semidefinite matrix. \mathbf{A}_i is referred to as the pricing-factor matrix of CR link i and $\mathbf{A}_i^{(k)}$ is referred to as the pricing-factor matrix at frequency band k of link i . The following theorem guarantees the existence of a NE of the game (10).

Theorem 1: There exists at least one NE for the noncooperative game in (10).

Proof: See Appendix I. □

The above game can have more than one NE. To guarantee a lower bound for the efficiency on the achieved NE, we propose in the next theorem a user-dependent pricing function. The proposed pricing policy ensures that at the resulting NE, the CRN throughput is at least as good as that of a locally optimal solution to the network optimization problem (6).

Theorem 2: For the game in (10) to converge to a NE at which the CRN's throughput equals to that of a locally optimal solution of problem (6), the pricing-factor matrix \mathbf{A}_i in (12) must have its k block matrix $\mathbf{A}_i^{(k)}$ of the following form:

$$\mathbf{A}_i^{(k)} = \sum_{j \in \Phi_N \setminus \{i\}} \mathbf{H}_{d(j),i}^{(k)H} \mathbf{C}_{d(j)}^{(k)-1} \mathbf{H}_{d(j),j}^{(k)} [(\tilde{\mathbf{T}}_j^{(k)} \tilde{\mathbf{T}}_j^{(k)H})^{-1} + \mathbf{H}_{d(j),j}^{(k)H} \mathbf{C}_{d(j)}^{(k)-1} \mathbf{H}_{d(j),j}^{(k)}]^{-1} \mathbf{H}_{d(j),j}^{(k)H} \mathbf{C}_{d(j)}^{(k)-1} \mathbf{H}_{d(j),i}^{(k)} \quad (13)$$

Proof: See Appendix II. □

To compute the pricing-factor matrix \mathbf{A}_i in (12), a CR transmitter i needs to obtain feedback regarding the interference-plus-noise covariance, the precoding, and the channel matrices from all other links. In practice, if the channel gain matrix from i to $d(j)$ is too weak, i.e., $\mathbf{H}_{d(j),i}^{(k)} \approx \mathbf{0}$, there is no need for $d(j)$ to send its feedback to i . Hence, i only gets feedback from receivers $d(j)$ that are within i 's vicinity. It is also worth noting that the feedback information is locally available at a receiver $d(j)$ as a byproduct of its decoding process (i.e., successive interference cancelation (SIC) receivers [3]). The k th block $\mathbf{A}_i^{(k)}$ of the pricing factor matrix in (13) agrees with that has been derived in [14] for a single-band MIMO CRN using first order Taylor series approximation. That is because we assume that all bands are orthogonal. However, in our case, the pricing matrix is a block diagonal matrix. Additionally, the necessary conditions of $\mathbf{A}_i^{(k)}$ have not been derived in the single-band case. How a MAC protocol design can support the computation of the above pricing-factor matrix at a node will be discussed shortly.

C. Best Response: Optimal Antenna Radiation Directions and Power Allocation

We now solve the individual utility optimization problem (10), from which a CR user finds its best response given the actions of other CR links. Noting that problem (10) is convex, hence can be solved by standard methods, e.g., interior point [26], requiring polynomial time w.r.t to the problem's number of variables. Authors in [11] solved a similar problem using semidefinite programming. However, as mentioned before, the number of variables of (10) grows quadratically with the number of antennas and can be very large. In this section, we develop an efficient algorithm whose complexity is independent to the antenna array size. It should also be noted that using our proposed pricing policy, the per-user optimization problem cannot be solved by water filling algorithms in [19] [20] as the optimal precoding matrix does not necessarily diagonalize the pricing-factor matrix in (10).

Recalling the convexity of (10) and that the Slater's conditions can easily be shown to hold [27], strong duality holds for problem (10), i.e., an optimal solution $\tilde{\mathbf{T}}_i$ to (10) should also solve the following dual problem (as in the case of a single-channel MIMO network [14]):

$$\text{DP : } \underset{\{\alpha_i^{(k)}, \gamma_i \geq 0, \forall k \in \Psi_K\}}{\text{minimize}} \quad D(\alpha_i^{(k)}, \gamma_i) \quad (14)$$

where $D(\alpha_i^{(k)}, \gamma_i)$ is the dual function, defined as:

$$D(\alpha_i^{(k)}, \gamma_i) = \underset{\{\tilde{\mathbf{T}}_i^{(k)}, \forall k \in \Psi_K\}}{\text{maximize}} \quad L_i(\tilde{\mathbf{T}}_i, \alpha_i^{(k)}, \gamma_i). \quad (15)$$

with $L_i(\tilde{\mathbf{T}}_i, \alpha_i^{(k)}, \gamma_i)$ is the Lagrangian function defined in (30).

The optimal matrix $\tilde{\mathbf{T}}_i$ of (10) is featured in the following theorem.

Theorem 3: The $M \times KM$ block matrix $\tilde{\mathbf{T}}_i$ that solves the individual utility optimization problem (or the user's best response) must have its k th block, the matrix $\tilde{\mathbf{T}}_i^{(k)}$, in a form of the generalized eigen matrix of the matrix $\mathbf{H}_{d(i),i}^{(k)H} \mathbf{C}_{d(i)}^{(k)-1} \mathbf{H}_{d(i),i}^{(k)}$ and matrix $\mathbf{A}_i^{(k)} + (\alpha_i^{(k)} + \gamma_i) \mathbf{I}$, where $\alpha_i^{(k)}$ and γ_i are the optimal Lagrange

multipliers of (10). In other words, the following equations must hold $\forall k \in \Psi_K$:

$$\mathbf{H}_{d(i),i}^{(k)H} \mathbf{C}_{d(i)}^{(k)-1} \mathbf{H}_{d(i),i}^{(k)} \tilde{\mathbf{T}}_i^{(k)} = [\mathbf{A}_i^{(k)} + (\alpha_i^{(k)} + \gamma_i) \mathbf{I}] \tilde{\mathbf{T}}_i^{(k)} \mathbf{\Lambda}_i^{(k)} \quad (16)$$

where $\mathbf{\Lambda}_i^{(k)}$ is a given $M \times M$ diagonal matrix.

Proof: See Appendix III. □

As previously discussed, the precoding matrix $\tilde{\mathbf{T}}_i^{(k)}$ determines both the directions of the antenna radiation as well as how node i allocates its transmission power on different antennas over frequency band k . Theorem (3) states a class of matrices that the solution of (10) must belong to. This class provides the directions that a user i should point its antenna radiation to.

The next step is to find the optimal power allocation $P_{s,k}^{(i)}$ for the set of KM data streams. To ensure that $\tilde{\mathbf{T}}_i^{(k)}$ belongs to the class of matrices specified by Theorem (3), we let:

$$\tilde{\mathbf{T}}_i^{(k)} = \mathbf{T}_i^{(k)} \times \mathbf{P}_k^{(i)1/2} \quad (17)$$

where $\mathbf{T}_i^{(k)}$ is an $M \times M$ matrix with unit-norm column vectors that satisfies (16). This matrix can be found by normalizing the generalized eigen matrix $\tilde{\mathbf{T}}_i^{(k)}$. $\mathbf{P}_k^{(i)1/2}$ is a square root matrix of the $M \times M$ diagonal matrix $\mathbf{P}_k^{(i)}$ whose diagonal entry (s, s) is the power allocated to sub-channel (s, k) , $P_{s,k}^{(i)}$. We can verify that the expression of $\tilde{\mathbf{T}}_i^{(k)}$ in (17) satisfies (16).

As $\tilde{\mathbf{T}}_i^{(k)}$ is a generalized eigen matrix of matrices $\mathbf{H}_{d(i),i}^{(k)H} \mathbf{C}_{d(i)}^{(k)-1} \mathbf{H}_{d(i),i}^{(k)}$ and $\mathbf{A}_i^{(k)} + (\alpha_i^{(k)} + \gamma_i) \mathbf{I}$, then $\mathbf{T}_i^{(k)}$ must also diagonalize each of the two matrices [28]:

$$\mathbf{T}_i^{(k)H} [\mathbf{H}_{d(i),i}^{(k)H} \mathbf{C}_{d(i)}^{(k)-1} \mathbf{H}_{d(i),i}^{(k)}] \mathbf{T}_i^{(k)} = \mathbf{\Pi}_i^{(k)} \quad (18)$$

$$\mathbf{T}_i^{(k)H} [\mathbf{A}_i^{(k)} + (\alpha_i^{(k)} + \gamma_i) \mathbf{I}] \mathbf{T}_i^{(k)} = \mathbf{\Omega}_i^{(k)} \quad (19)$$

where $\mathbf{\Pi}_i^{(k)}$ and $\mathbf{\Omega}_i^{(k)}$ are $M \times M$ diagonal matrices.

Note that though its columns have unit-norm, $\mathbf{T}_i^{(k)}$ is not an orthonormal matrix as $\mathbf{A}_i^{(k)}$ is generally not similar to \mathbf{I} . Hence, $\mathbf{T}_i^{(k)}$ (then $\tilde{\mathbf{T}}_i^{(k)}$) does not diagonalize $\mathbf{A}_i^{(k)}$. This observation is twofold. First, this

points out that the the solution to the problem in [21] was incorrectly derived. Second, though the optimal power allocation over KM data streams problem seems very similar to a general water filling problem [19] with multiple water levels (one water level per each frequency band), it cannot be solved by the algorithm developed in [19]. This is because $\tilde{\mathbf{T}}_i^{(k)}$ does not diagonalize $\mathbf{A}_i^{(k)}$ in (10), hence we cannot convert (10) to a general water filling problem.

Plugging (18) and (19) into the Lagrangian function (30), we have:

$$L_i(\tilde{\mathbf{T}}_i, \alpha_i^{(k)}, \gamma_i) = \sum_{k \in \Psi_K} \left\{ \sum_{s=1}^M \{ \log(1 + P_{s,k}^{(i)} \text{diag}_s(\mathbf{\Pi}_i^{(k)}) - P_{s,k}^{(i)} \text{diag}_s(\mathbf{\Omega}_i^{(k)}) \} + \alpha_i^{(k)} P_{\text{mask}}(f_k) + \frac{\gamma_i}{K} P_{\text{max}} \right\}. \quad (20)$$

The optimal power allocation $P_{s,k}^{(i)}$ is obtained by equating the derivative of the Lagrangian (20) w.r.t $P_{s,k}^{(i)}$ to zero:

$$\frac{\partial L_i(\tilde{\mathbf{T}}_i, \alpha_i^{(k)}, \gamma_i)}{\partial P_{s,k}^{(i)}} = \frac{\text{diag}_s(\mathbf{\Pi}_i^{(k)})}{1 + P_{s,k}^{(i)} \text{diag}_s(\mathbf{\Pi}_i^{(k)})} - \text{diag}_s(\mathbf{\Omega}_i^{(k)}) = 0 \quad (21)$$

Thus:

$$P_{s,k}^{(i)} = \max \left(0, \frac{\text{diag}_s(\mathbf{\Pi}_i^{(k)}) - \text{diag}_s(\mathbf{\Omega}_i^{(k)})}{\text{diag}_s(\mathbf{\Pi}_i^{(k)}) \text{diag}_s(\mathbf{\Omega}_i^{(k)})} \right) \quad (22)$$

Plugging (22) into (20), we obtain the dual function:

$$D(\alpha_i^{(k)}, \gamma_i) = \sum_{k \in \Psi_K} \left\{ \sum_{s=1}^M \left\{ \log \frac{\text{diag}_s(\mathbf{\Pi}_i^{(k)})}{\text{diag}_s(\mathbf{\Omega}_i^{(k)})} - 1 + \frac{\text{diag}_s(\mathbf{\Omega}_i^{(k)})}{\text{diag}_s(\mathbf{\Pi}_i^{(k)})} \right\} + \alpha_i^{(k)} P_{\text{mask}}(f_k) + \frac{\gamma_i}{K} P_{\text{max}} \right\} \quad (23)$$

$$\forall s, k \text{ such that } \text{diag}_s(\mathbf{\Pi}_i^{(k)}) > \text{diag}_s(\mathbf{\Omega}_i^{(k)}) > 0.$$

To solve the DP (14) for $\alpha_i^{(k)}$ and γ_i , we note that the problem is convex, hence, any stationary point is a globally optimal solution. Moreover, as the objective function and constraints of the primal problem (10) is continuous w.r.t every entry of $\tilde{\mathbf{T}}_i$, the dual function $D(\alpha_i^{(k)}, \gamma_i)$ is differentiable w.r.t $\alpha_i^{(k)}$ and γ_i [26]. Hence, a gradient algorithm can be used to obtain the optimal Lagrangian multipliers $\alpha_i^{(k)}$ and γ_i by searching for a stationary point of the augmented Lagrangian of DP. It should be noted that even if the dual

function is not differentiable (i.e., multiple subgradients may exist), a subgradient-based search algorithm with appropriate step size can still be used to converge to the optimal point [26]. The augmented Lagrangian of DP is given by:

$$\begin{aligned}
& L(\alpha_i^{(k)}, \gamma_i, p, \lambda^{(k)}) \\
& = D(\alpha_i^{(k)}, \gamma_i) + \frac{p}{2} \{(\max\{0, \lambda^{(1)} - p\gamma_i\})^2 - (\lambda^{(1)})^2\} + \frac{p}{2} \sum_{k \in \Psi_K} \{(\max\{0, \lambda^{(k+1)} - p\alpha_i^{(k)}\})^2 - (\lambda^{(k+1)})^2\}
\end{aligned} \tag{24}$$

where p is a positive penalty parameter (for violating the constraints) and $\lambda^{(k)}$'s are nonnegative Lagrangian multipliers.

Our gradient algorithm uses Armijo step with steepest descent direction. This search mechanism together with the above analysis are summarized in Algorithm 1. We emphasize that by exploiting the strong duality, this algorithm needs only to deal with $K + 1$ variables, instead of $2KM^2$ variables of the primal problem (10).

Although the individual optimization (10) is to be solved distributedly at each node, at the achieved NE, network throughput is analytically guaranteed to be as good as that of a locally optimal point of the network optimization problem (6). Before developing a centralized algorithm that serves as a simulation's performance benchmark, let's briefly discuss how a MAC protocol can implement the Algorithm 1 and its convergence behavior.

D. A MAC Protocol

Using either a dedicated control channel or some frequency hopping mechanism to establish an initial dialogue, a MAC protocol that executes the distributed Algorithm 1 can be designed. This protocol divides the time axis into three windows: *Access window*, *training window*, and *data window*. The access window is dedicated to CR nodes that have data to send. These nodes first exchange some initial rendezvous packets (e.g., RTS and CTS). Unlike IEEE 802.11, our MAC design does not use RTS/CTS packets to silence nearby nodes to reserve the transmission floor for the coming transmission. Instead, we use these signalling

Algorithm 1 Distributed Algorithm for the Power Allocation and Spectrum Management Game

```

1: Input:
    $\tilde{\mathbf{T}}_{-i} = [\tilde{\mathbf{T}}_1(t+1), \dots, \tilde{\mathbf{T}}_{i-1}(t+1), \tilde{\mathbf{T}}_{i+1}(t), \dots, \tilde{\mathbf{T}}_N(t)]$  with Gauss-Seidel iteration
    $\tilde{\mathbf{T}}_{-i} = [\tilde{\mathbf{T}}_1(t), \dots, \tilde{\mathbf{T}}_{i-1}(t), \tilde{\mathbf{T}}_{i+1}(t), \dots, \tilde{\mathbf{T}}_N(t)]$ 
   with Jacobi iteration
2: Initialize
    $\tilde{\mathbf{T}}_i^{(k)}(t+1) \leftarrow \tilde{\mathbf{T}}_i^{(k)}(t), \gamma_i \leftarrow 0; \alpha_i^{(k)} \leftarrow 0, \forall k \in \Psi_K$ 
3: while true do
4:    $\beta \leftarrow .7, \sigma \leftarrow .1$  %used in Armijo search
5:    $\lambda^{(k)} \leftarrow .1 \forall k = 1 \dots (K+1)$ 
6:    $p \leftarrow 1$ 
7:   while  $\partial L(\alpha_i^{(k)}, \gamma_i, p, \lambda^{(k)}) \neq 0$  do
8:      $step \leftarrow 0.1$ 
9:      $D \leftarrow \partial L(\alpha_i^{(k)}, \gamma_i, p, \lambda^{(k)})$ 
10:     $d \leftarrow -step \times D; m \leftarrow 0$ 
11:    {Find Armijo step size}
12:    while  $L(\alpha_i^{(k)}, \gamma_i, p, \lambda^{(k)}) - L(\alpha_i^{(k)} + d, \gamma_i + d, p, \lambda^{(k)}) \leq -\sigma \beta^m step \partial LD$  do
13:       $step \leftarrow step \times \beta; m \leftarrow m + 1$ 
14:       $d \leftarrow -step \times D$ 
15:    end while
16:     $\alpha_i^{(k)} \leftarrow \alpha_i^{(k)} + d, \gamma_i \leftarrow \gamma_i + d$ 
17:  end while
18:  if  $\min(\alpha_i^{(k)}, \gamma_i, \forall k \in \Psi_K) \geq 0$  break
19:   $\forall k \in \Psi_K :$ 
20:   $\lambda^{(k)} \leftarrow \lambda^{(k)} - p\alpha_i^{(k)}$  if  $\lambda^{(k)} - p\alpha_i^{(k)} > 0$  else  $\lambda^{(k)} = 0$ 
21:   $\lambda^{(1)} \leftarrow \lambda^{(1)} - p\gamma_i$  if  $\lambda^{(1)} - p\gamma_i \geq 0$  else  $\lambda^{(1)} = 0$ 
22:   $p \leftarrow p \times \mu$  % $\mu \geq 1$ , increase cost of violation
23: end while
24: Plug  $\gamma_i, \alpha_i^{(k)}$  into (16) (Theorem 3) to find  $\mathbf{T}_i^{(k)}$ 
    $\mathbf{P}_k^{(i)}$  is found from (18), (19), (22).  $\tilde{\mathbf{T}}_i^{(k)}$  is found from (17).
25: RETURN  $\tilde{\mathbf{T}}_i^{(k)}(t+1), \forall k \in \Psi_K$  at time  $(t+1)$ 

```

packets handshake a number of node pairs. After this phase, several pairs of CR users communicate during the training window, whose purpose is to exchange/negotiate transmit strategies (precoding matrices). The signalling packets in either the access or transmit windows can also be used to embed training sequences to obtain channel gain matrices. The data window then follows with multiple DATA packets sent using negotiated transmission strategies. The mechanism is referred to as a flow-based one in [2].

To reduce the feedback overhead in the training window, one may relax the time scale of recalculating the pricing-factor matrix. This represents a tradeoff between throughput and feedback freshness. One can even omit the training window by having nodes to embed updating information into every DATA and ACK packet. Then, upon receiving an ACK for each DATA packet sent, a transmitter recomputes its pricing-factor matrix. This method is referred to as a packet-based one where less overhead and lower delay are sustained at the expense of network throughput and convergence speed [29] [2].

An important issue for protocol designers is how to set the size of the training window. That depends

on the convergence speed of the updating process. To ensure that the training window is not too long, the updating and negotiation processes must converge. During the training window, a node can use either Gauss-Seidel (sequential) or Jacobi (parallel) iterations (see Algorithm 1) to update its precoding matrices. Though we cannot prove the convergence under the Jacobi iteration, simulations show that the distributed algorithm converges faster with Jacobi iterations than Gauss-Seidel (less than nine iterations for about ten links in Figure 5). The convergence behavior under the Gauss-Seidel iteration is claimed in the following theorem.

Theorem 4: Under the sequential updating procedure (Gauss-Seidel), the distributed Algorithm 1 drives the game (10) to its NE.

Proof: See Appendix IV. □

In [20] [18], the authors converted the throughput maximization game (of a single-frequency MIMO CRN) into a *variational inequality* problem (see [30] and therein references for a tutorial on variational inequality theory) for the purpose of providing the convergence and uniqueness conditions of a NE. Intuitively, the game converges to a unique NE if there is not too much interference at a receiver and all channel matrices are full column-rank. The former requires transmitters to adjust its transmission parameters and the latter is uncertain and cannot be always guaranteed. However, using our proposed pricing policy and the Gauss-Seidel procedure, the game (10) always converges to a NE without requiring transmitters and channel matrices to meet any additional condition. Regarding the uniqueness of the NE, our game may have more than one NEs, however the performance at any achieved NE is always bounded from below by that of a locally optimal solution of the network optimization problem.

Both Gauss-Seidel and Jacobi updating procedures are *synchronous* ones that require CR nodes have to be in synch. This may not be always feasible as CRs are spatially distributed. By contrast, *asynchronous* update procedures refer to cases where some players at some iterations do not update others their strategies (e.g., due to collisions). Using variational inequality theory, the mean-value theorem, and follow the routine in [18], we provide conditions under which the game (10) converge to a unique NE under either synchronous or asynchronous updates (we omit detailed manipulation due to space limit).

Theorem 5: The game (10) always converges to a unique NE if all channel matrices are full column-rank and the spectrum radius of matrix $J^{-1}\Gamma$ less than 1:

$$\text{radius}(J^{-1}\Gamma) < 1$$

where

$$J \stackrel{\text{def}}{=} \begin{bmatrix} \sigma_1 & 0 & \dots & 0 \\ 0 & \sigma_2 & \dots & 0 \\ \vdots & \vdots & \ddots & \vdots \\ 0 & 0 & \dots & \sigma_N \end{bmatrix} \quad \Gamma \stackrel{\text{def}}{=} \begin{bmatrix} 0 & \kappa_{1,2} & \dots & \kappa_{1,N} \\ \kappa_{2,1} & 0 & \dots & \kappa_{2,N} \\ \vdots & \vdots & \ddots & \vdots \\ \kappa_{N,1} & \kappa_{N,2} & \dots & 0 \end{bmatrix}$$

and

$$\sigma_i \stackrel{\text{def}}{=} \min_{k \in \Psi_K} \left(\text{eig}_{\min}^2 \left(\mathbf{H}_{d(i),i}^{\{k\}H} \left(\mathbf{I} + \sum_{j \in \Phi_N} P_{\text{mask}}(f_k) \mathbf{H}_{d(j),i}^{\{k\}} \mathbf{H}_{d(j),i}^{\{k\}H} \right)^{-1} \mathbf{H}_{d(i),i}^{\{k\}} \right) \right)$$

$$\kappa_{j,i} \stackrel{\text{def}}{=} \max_{k \in \Psi_K} \left(\text{eig}_{\max} \left(\mathbf{H}_{d(j),i}^{\{k\}} \mathbf{H}_{d(j),i}^{\{k\}H} \right) \text{eig}_{\max} \left(\mathbf{H}_{d(i),i}^{\{k\}} \mathbf{H}_{d(i),i}^{\{k\}} \right) \right) \quad \forall i \neq j \in \Psi_N$$

with $\text{eig}_{\min}(\cdot)$ and $\text{eig}_{\max}(\cdot)$ operators yield the smallest and largest eigenvalues of a matrix (\cdot) , respectively.

V. CENTRALIZED ALGORITHM

From a game theoretic perspective, a centralized algorithm can be obtained by formulating the problem as a cooperative game, where a network operator somehow controls the behaviors of all players in order to maximize the network throughput (total payoff). In this section, we use the augmented Lagrangian multiplier method to derive such a centralized algorithm.

We rewrite network-wide problem (6) as follows:

$$\begin{aligned} & \underset{\{\tilde{\mathbf{T}}_i^{(k)}, \forall k \in \Psi_K, \forall i \in \Phi_N\}}{\text{minimize}} && - \sum_{i \in \Phi_N} R(i) \\ & \text{s.t.} && \\ & c_i = \sum_{k \in \Psi_K} \text{tr}(\tilde{\mathbf{T}}_i^{(k)} \tilde{\mathbf{T}}_i^{(k)H}) - P_{\text{max}} \leq 0 \quad \forall i \in \Phi_N && \\ & c_{k,i} = \text{tr}(\tilde{\mathbf{T}}_i^{(k)} \tilde{\mathbf{T}}_i^{(k)H}) - P_{\text{mask}}(f_k) \leq 0 \quad \forall k \in \Psi_K, \forall i \in \Phi_N && \end{aligned} \tag{25}$$

The augmented Lagrangian of (25) is given by [26]:

$$\begin{aligned}
& L(\tilde{\mathbf{T}}, \alpha_i^{(k)}, \gamma_i, p) \\
&= - \sum_{i \in \Phi_N} R_{(i)} + \frac{p}{2} \sum_{i \in \Phi_N} \{(\max\{0, \gamma_i + pc_i\})^2 - (\gamma_i)^2\} + \frac{p}{2} \sum_{i \in \Phi_N} \sum_{k \in \Psi_K} \{(\max\{0, \alpha_i^{(k)} + pc_{k,i}\})^2 - (\alpha_i^{(k)})^2\}
\end{aligned} \tag{26}$$

where p is a positive penalty parameter (for violating the constraints), and $\alpha_i^{(k)}$ and γ_i are nonnegative Lagrangian multipliers.

At a locally optimal solution, we have:

$$0 = \frac{\partial L(\tilde{\mathbf{T}}, \alpha_i^{(k)}, \gamma_i, p)}{\partial \tilde{\mathbf{T}}_i^{(k)*}} = - \sum_{j \in \Phi_N \setminus \{i\}} \frac{\partial R_j^{(k)}}{\partial \tilde{\mathbf{T}}_i^{(k)*}} - \frac{\partial R_i^{(k)}}{\partial \tilde{\mathbf{T}}_i^{(k)*}} + \frac{p}{2} \left\{ \frac{\partial \{(\max\{0, \gamma_i + pc_i\})^2\}}{\partial \tilde{\mathbf{T}}_i^{(k)*}} + \frac{\partial \{(\max\{0, \alpha_i^{(k)} + pc_{k,i}\})^2\}}{\partial \tilde{\mathbf{T}}_i^{(k)*}} \right\} \tag{27}$$

The first term in (27) is computed in (35). Its second term is given as:

$$\frac{\partial R_i^{(k)}}{\partial \tilde{\mathbf{T}}_i^{(k)*}} = \mathbf{H}_{d(i),i}^{(k)H} (\mathbf{C}_{d(i)}^{(k)} + \mathbf{H}_{d(i),i}^{(k)} \tilde{\mathbf{T}}_i^{(k)} \tilde{\mathbf{T}}_i^{(k)H} \mathbf{H}_{d(i),i}^{(k)H})^{-1} \mathbf{H}_{d(i),i}^{(k)} \tilde{\mathbf{T}}_i^{(k)}. \tag{28}$$

Since c_i and $c_{k,i}$ are continuously differentiable w.r.t every entry of $\tilde{\mathbf{T}}$, the third and fourth terms in (27) are also continuously differentiable [26]. Their derivatives are as follows:

$$\begin{aligned}
\frac{\partial \{(\max\{0, \gamma_i + pc_i\})^2\}}{\partial \tilde{\mathbf{T}}_i^{(k)*}} &= \begin{cases} 0 & \text{if } \gamma_i + pc_i \leq 0 \\ 2p(\gamma_i + pc_i) \tilde{\mathbf{T}}_i^{(k)} & \end{cases} \\
\frac{\partial \{(\max\{0, \alpha_i^{(k)} + pc_{k,i}\})^2\}}{\partial \tilde{\mathbf{T}}_i^{(k)*}} &= \begin{cases} 0 & \text{if } \alpha_i^{(k)} + pc_{k,i} \leq 0 \\ 2p(\alpha_i^{(k)} + pc_{k,i}) \tilde{\mathbf{T}}_i^{(k)} & \end{cases}
\end{aligned}$$

As mentioned earlier, because the network optimization problem is not convex, the centralized algorithm can only lead the network to operate at a locally optimal point. For that purpose, we use the gradient search algorithm with Armijo step size [26] to find $(\tilde{\mathbf{T}}, \alpha_i^{(k)}, \gamma_i, p)$ such that equation (27) holds for all frequency bands k and all users i . The details of the centralized algorithm is presented in Algorithm 2.

We emphasize that network throughput may vary from a locally optimal point to another. To account for such phenomenon, one can run the simulations multiple times with various starting points (initializations) and take the average of the achieved throughput. The running time of Algorithm 2 can be high, as it involves NKM^2 complex variables (or $2NKM^2$ real ones). To implement Algorithm 2, we use the following isomorphism mapping from a complex matrix to a vector of real variables. The vector of variables:

$$x = [(x_i^T)_{i=1}^N]^T$$

with $x_i = [\Re[\text{vec}(\tilde{\mathbf{T}}_i)]^T, \Im[\text{vec}(\tilde{\mathbf{T}}_i)]^T]^T = [\Re[\text{vec}(\tilde{\mathbf{T}}_i^{(1)})]^T, \dots, \Re[\text{vec}(\tilde{\mathbf{T}}_i^{(K)})]^T, \Im[\text{vec}(\tilde{\mathbf{T}}_i^{(1)})]^T, \dots, \Im[\text{vec}(\tilde{\mathbf{T}}_i^{(K)})]^T]^T$

The gradient of the corresponding Lagrangian is given by:

$$\nabla_x L = 2 \left[\Re[\text{vec}(\frac{\partial L}{\partial \tilde{\mathbf{T}}_1^{(1)*}})]^T, \dots, \Re[\text{vec}(\frac{\partial L}{\partial \tilde{\mathbf{T}}_N^{(K)*}})]^T, \Im[\text{vec}(\frac{\partial L}{\partial \tilde{\mathbf{T}}_1^{(1)*}})]^T, \dots, \Im[\text{vec}(\frac{\partial L}{\partial \tilde{\mathbf{T}}_N^{(K)*}})]^T \right]^T$$

Algorithm 2 Centralized Algorithm for the Social Optimization Problem (6)

```

1: Initialize
    $\tilde{\mathbf{T}}_i^{(k)} \leftarrow \mathbf{I}, \gamma_i \leftarrow 0; \alpha_i^{(k)} \leftarrow 0, \forall k \in \Psi_K, \forall i \in \Phi_N$ 
2: while true do
3:    $\beta \leftarrow .7, \sigma \leftarrow .1$  Used in Armijo search
4:    $\gamma_i \leftarrow 0, \alpha_i^{(k)} \leftarrow 0, \forall k \in \Psi_K, \forall i \in \Phi_N$ 
5:    $p \leftarrow 1$ 
6:   while  $\partial L(\tilde{\mathbf{T}}, \alpha_i^{(k)}, \gamma_i, p) \neq 0$  do
7:      $step \leftarrow 0.1$ 
8:      $D \leftarrow \partial L(\tilde{\mathbf{T}}, \alpha_i^{(k)}, \gamma_i, p)$ 
9:      $d \leftarrow -step \times D; m \leftarrow 0$ 
10:    {Find Armijo step size}
11:    while  $L(\tilde{\mathbf{T}}, \alpha_i^{(k)}, \gamma_i, p) - L(\tilde{\mathbf{T}} + d, \alpha_i^{(k)}, \gamma_i, p) \leq -\sigma \beta^m step \partial LD$  do
12:       $step \leftarrow step \times \beta; m \leftarrow m + 1$ 
13:       $d \leftarrow -step \times D$ 
14:    end while
15:     $\tilde{\mathbf{T}} \leftarrow \tilde{\mathbf{T}} + d$ 
16:  end while
17:  if  $\max(c_i, c_{i,k}, \forall k \in \Psi_K, \forall i \in \Phi_N) \leq 0$  break
18:   $\forall k \in \Psi_K, \forall i \in \Phi_N$  :
19:     $\gamma_i = \gamma_i + pc_i$  if  $\gamma_i + pc_i \geq 0$  else  $\gamma_i = 0$ 
20:     $\alpha_i^{(k)} = \alpha_i^{(k)} + pc_{k,i}$  if  $\alpha_i^{(k)} + pc_{k,i} \geq 0$  else  $\alpha_i^{(k)} = 0$ 
21:     $p \leftarrow p \times \mu$  if  $\mu \geq 1$ , increase cost of violation
22:  end while
23: RETURN  $\tilde{\mathbf{T}}_i^{(k)}, \forall k \in \Psi_K, \forall i \in \Phi_N$ 

```

VI. NUMERICAL RESULTS

In this section, we numerically evaluate the performance of the distributed algorithm using MATLAB-based simulations. We compare the network throughput of the distributed algorithm with the centralized one and with a greedy algorithm, in which nodes selfishly attempt to maximize their own rates. The greedy

algorithm is exactly the same as the distributed one except that its pricing-factor matrix A_i is a null matrix. Another algorithm called *uniform* is obtained by uniformly dividing a node's total transmit power over all available channels and then applying the single-band approach in [14] for each channel. We emphasize that this uniform algorithm does not meet the optimality conditions (33) of the network problem (6).

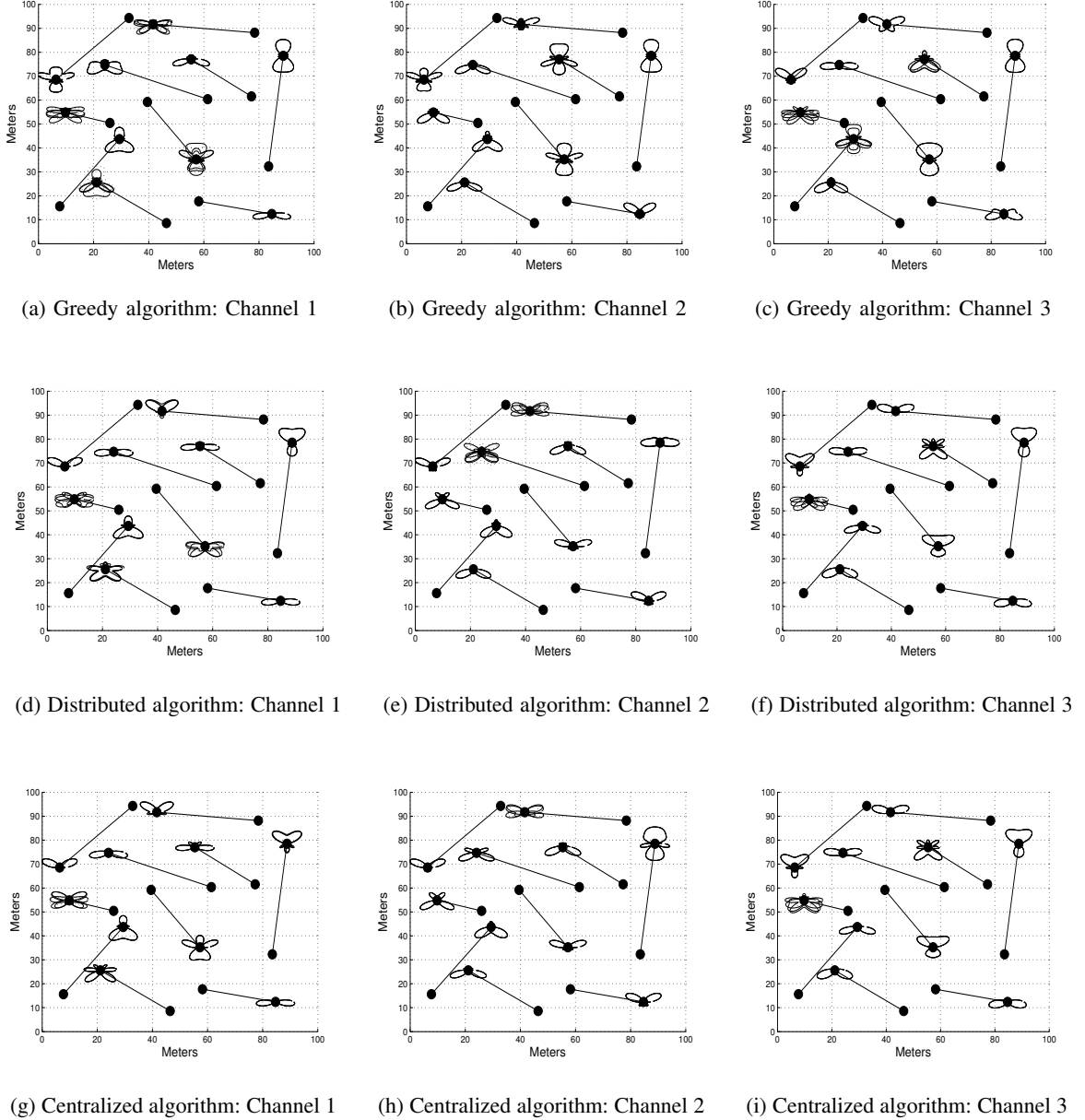


Fig. 3. Antenna radiation patterns under the greedy, distributed, and centralized algorithms.

Because the number of variables in the centralized algorithm is quite high ($2NKM^2$), its running time can be very long. Therefore, to compare the performances of the four algorithms, we consider a CRN of $N = 10$ links with $K = 3$ bands ($f_1 = 2.4$ GHz, $f_2 = 2.7$ GHz, and $f_3 = 3$ GHz with identical channel

bandwidth of 1 MHz), and antenna array size $M = 4$. The results are averaged over 30 runs. In each run, N links are randomly placed in a 100 meter \times 100 meter square. The maximum power at each node is $2W$ and the power mask is $0.8W$ on all frequency bands. The channel fading is flat with free-space attenuation factor of 2. The spreading angles of the signal at the receive antennas range from $-\pi/5$ to $\pi/5$. For the lowest frequency, we assume that the received power at a reference distance of 100 meters reduces 10 dB compared with the transmit power. To account for the frequency-dependent attenuation factor, we assume that the received power at the reference distance decreases 2 dB more if the frequency increases by 300 MHz. As mentioned before, the noise from PR transmissions is treated as floor noise that together with the thermal noise are normalized to a unit variance. The initializations of the precoding matrices are different for all algorithms.

A snapshot of the network topology and antenna radiation patterns (at the converged points) over different frequencies is shown in Figure 3. We can visually note that the transmitters under the distributed and centralized algorithms often steer their beams away from neighboring receivers. This results from attempting to minimize the price function (11). It can also be seen that the antenna patterns of the distributed and centralized algorithms are very similar, suggesting the two algorithms may converge to the same point.

Figure 4 depicts the network throughput under four algorithms (distributed, centralized, greedy, and uniform) versus the number of iterations. Though the network performance at the converged points for the distributed and centralized algorithms change with their starting points, after averaging over multiple runs with different initializations, the throughput of the distributed algorithm is almost the same as that of the centralized one. We also notice that, by using the proposed pricing policy to regulate interference, the distributed algorithm almost doubles the network throughput compared with the greedy algorithm. The uniform algorithm also improves network throughput over the greedy one but it remains inferior to the distributed algorithm. This is because the uniform algorithm evenly allocates its power over all available channels and does not optimize over the frequency dimension, while the distributed algorithm attempts to optimize the antenna radiation patterns and the power allocation over both space and frequency.

To evaluate the energy efficiency of the four algorithms, we record the average power consumption and

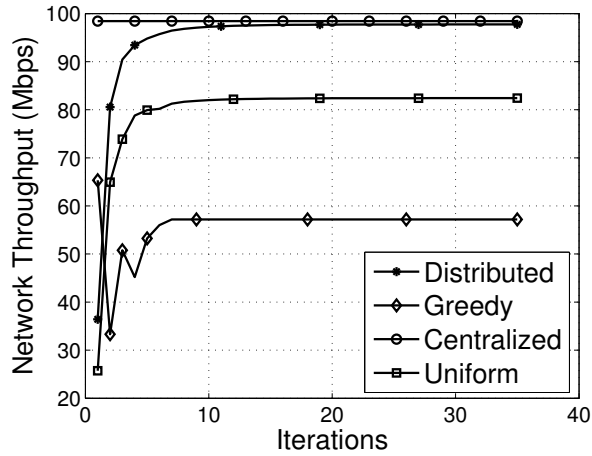


Fig. 4. Network throughput vs. iterations.

power allocation over all nodes and all run in Table I. As shown in Table I, without regulating interference, nodes under the greedy algorithm selfishly compete for their own throughput by always using their maximum power ($2W$), leading to the highest power consumption among the four algorithms. The power consumption for the distributed algorithm is comparable to that of the centralized and uniform algorithms, and 10% less than that of the greedy one. Power allocation over both space and frequency at a representative node under the distributed algorithm is shown in Table II. From Tables I and II, we note that the inequality constraints in problems (10) and (6) are not active at their solutions. That is because transmitting at high power may be expensive due to the proposed pricing method.

Channels	Centralized	Greedy	Distributed	Uniform
f_1	0.768	0.71	0.76	0.658
f_2	0.643	0.66	0.61	0.556
f_3	0.422	0.63	0.44	0.627
Total (W)	1.823	2.00	1.81	1.831

TABLE I

AVERAGE POWER CONSUMPTION AND POWER ALLOCATION OVER DIFFERENT CHANNELS (IN WATTS).

Antennas	f_1	f_2	f_3
1	0.135	0.085	$0.15e - 10$
2	0.209	0.386	0.02
3	0.550	0.314	$0.06e - 10$
4	0.194	0.035	0.305
Total=1.913(W)	0.788	0.8	0.325

TABLE II

POWER ALLOCATION AT A NODE OVER SPACE AND FREQUENCY DIMENSIONS UNDER THE DISTRIBUTED ALGORITHM (IN WATTS).

We say that the algorithm converges if the change in the throughput of one iteration (relative to the previous iteration) is less than a given threshold (i.e., 3%). The convergence speed of the distributed algorithm versus the number of links is shown in Figure 5.

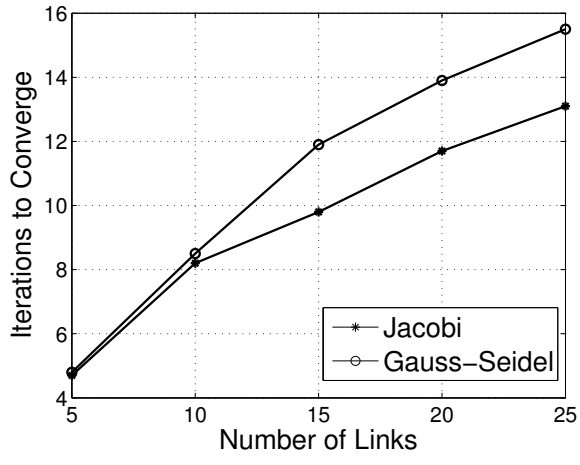


Fig. 5. Convergence speed of the distributed algorithm.

Figure 6 depicts the network throughput under the distributed and greedy algorithms versus the number of links using Jacobi update policy. The distributed algorithm consistently improves the throughput over the greedy one. The improvement becomes more significant with a higher number of links. That is because as the node density increases (higher number of links), network interference increases. Interference management becomes more critical and more impact on throughput.

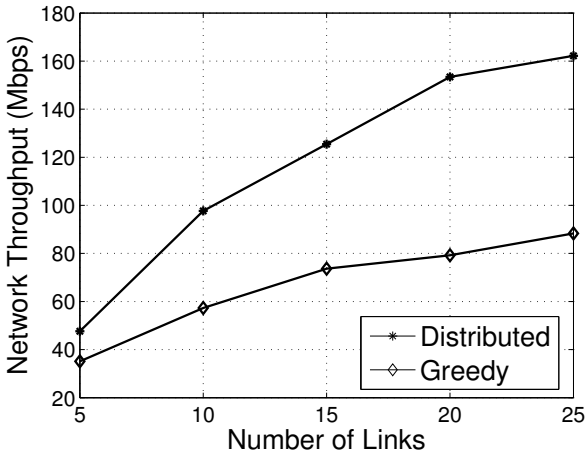


Fig. 6. Network throughput vs. the number of links.

VII. CONCLUSIONS

In this work, we investigated the spectrum sharing problem in multi-antenna CRNs. By adjusting the precoding matrices, we allocate power over both the frequency and space dimensions while managing the antenna's radiation beams to reduce network interference, aiming at maximizing the network throughput. Using game theory and the strong duality in convex optimization, we designed a low-complexity distributed algorithm and its corresponding MAC protocol that achieve the same throughput as a locally optimal point of the non-convex centralized network problem. The key idea behind the algorithm is the introduction of a diagonal block pricing-factor matrix for each CR. This matrix regulates network interference by encouraging CRs to work in a cooperative manner. Simulations showed that the proposed algorithm dramatically improves network throughput and achieves higher energy efficiency, compared with existing solutions.

REFERENCES

- [1] W. Wang, Y. Cui, T. Peng, and W. Wang, "Noncooperative power control game with exponential pricing for cognitive radio network," in *Proceedings of the IEEE 65th Vehicular Technology Conference*, April 2007.
- [2] F. Wang, M. Krunz, and S. Cui, "Price-based spectrum management in cognitive radio networks," *IEEE Journal of Selected Topics in Signal Processing*, vol. 2, no. 1, pp. 74–87, 2008.
- [3] D. Tse and P. Viswanath, *Fundamentals of Wireless Communication*. Cambridge University Press, May 2005.
- [4] K. Sundaresan, R. Sivakumar, M. Ingram, and T.-Y. Chang, "A fair medium access control protocol for ad-hoc networks with MIMO links," in *Proceedings of the INFOCOM Conference*, vol. 4, March 2004, pp. 2559–2570.
- [5] K. Sundaresan and R. Sivakumar, "Routing in ad-hoc networks with MIMO links," in *Proceedings of the ICNP Conference*, Nov. 2005.
- [6] S. Chu and X. Wang, "Opportunistic and cooperative spatial multiplexing in MIMO ad hoc networks," in *Proceedings of MOBIHOC Conference*, 2008, pp. 63–72.
- [7] J. Liu, Y. Hou, Y. Shi, and H. Sherali, "On performance optimization for multi-carrier MIMO ad hoc networks," in *Proceedings of the ACM MOBIHOC Conference*, May 2009, pp. 43–54.
- [8] U. Phuyal, A. Punchihewa, V. Bhargava, and C. Despins, "Power loading for multicarrier cognitive radio with MIMO antennas," in *Proceedings of the IEEE Wireless Communications and Networking Conference (WCNC)*, April 2009, pp. 1–5.
- [9] R. Iltis, S.-J. Kim, and D. Hoang, "Noncooperative iterative MMSE beamforming algorithms for ad hoc networks," *IEEE Transactions on Communications*, vol. 54, no. 4, pp. 748–759, 2006.
- [10] C. Shi, R. Berry, and M. Honig, "Local interference pricing for distributed beamforming in MIMO networks," in *Proceedings of IEEE Military Communications Conference MILCOM*, 2009, pp. 1–6.

- [11] Y. J. Zhang and A. So, "Optimal spectrum sharing in MIMO cognitive radio networks via semidefinite programming," *IEEE Journal on Selected Areas in Communications*, vol. 29, no. 2, pp. 362–373, Feb. 2011.
- [12] D. Hoang and R. Iltis, "Noncooperative eigencoding for MIMO ad hoc networks," *IEEE Transactions on Signal Processing*, vol. 56, no. 2, pp. 865–869, 2008.
- [13] R. Zhang and Y.-C. Liang, "Exploiting multi-antennas for opportunistic spectrum sharing in cognitive radio networks," *IEEE Journal of Selected Topics in Signal Processing*, vol. 2, no. 1, pp. 88–102, Feb. 2008.
- [14] S.-J. Kim and G. B. Giannakis, "Optimal resource allocation for MIMO ad hoc cognitive radio networks," *IEEE Transactions on Information Theory*, vol. 57, no. 5, pp. 3117–3131, May 2011.
- [15] G. Scutari and D. Palomar, "MIMO cognitive radio: a game theoretical approach," *IEEE Transactions on Signal Processing*, vol. 58, no. 2, pp. 761–780, Feb. 2010.
- [16] Z. Tian, G. Leus, and V. Lottici, "Joint dynamic resource allocation and waveform adaptation for cognitive networks," *IEEE Journal on Selected Areas in Communications*, vol. 29, no. 2, pp. 443–454, Feb. 2011.
- [17] H. Salameh, M. Krunz, and O. Younis, "MAC protocol for opportunistic cognitive radio networks with soft guarantees," *IEEE Transactions on Mobile Computing*, vol. 8, no. 10, pp. 1339–1352, Oct. 2009.
- [18] J. Wang, G. Scutari, and D. Palomar, "Robust MIMO cognitive radio via game theory," *IEEE Transactions on Signal Processing*, vol. 59, no. 3, pp. 1183–1201, March 2011.
- [19] D. Palomar and J. Fonollosa, "Practical algorithms for a family of waterfilling solutions," *IEEE Transactions on Signal Processing*, vol. 53, no. 2, pp. 686–695, Feb 2005.
- [20] G. Scutari, D. Palomar, and S. Barbarossa, "Asynchronous iterative water-filling for gaussian frequency-selective interference channels," *IEEE Transactions on Information Theory*, vol. 54, no. 7, pp. 2868–2878, July 2008.
- [21] X. Dong, Y. Rong, and Y. Hua, "Cooperative power scheduling for a network of MIMO links," *IEEE Transactions on Wireless Communications*, vol. 9, no. 3, pp. 939–944, March 2010.
- [22] M. J. Osborne, *An Introduction to Game Theory*. Oxford University Press, 2004.
- [23] J. Hirshleifer, A. Glazer, and D. Hirshleifer, *Price Theory and Applications Decisions, Markets, and Information*. Cambridge University Press, 2005.
- [24] C. Saraydar, N. Mandayam, and D. Goodman, "Efficient power control via pricing in wireless data networks," *IEEE Transactions on Communications*, vol. 50, no. 2, pp. 291–303, Feb. 2002.
- [25] W. Yu, "Competition and cooperation in multi-user communication environments," *PhD Thesis, Stanford University, Stanford, CA*, 2002.
- [26] D. P. Bertsekas, *Nonlinear Programming*. Athena Scientific, 1995.
- [27] S. Boyd and L. Vandenberghe, *Convex Optimization*. Cambridge University Press, 2004.
- [28] R. A. Horn and C. R. Johnson, *Matrix Analysis*. Cambridge University Press, 1990.
- [29] R. Maheswaran and T. Basar, "Decentralized network resource allocation as a repeated noncooperative market game," in *Proceedings of the 40th IEEE Conference on Decision and Control*, vol. 5, 2001, pp. 4565–4570.

- [30] G. Scutari, D. Palomar, F. Facchinei, and J.-S. Pang, “Convex optimization, game theory, and variational inequality theory,” *IEEE Signal Processing Magazine*, May 2010.
- [31] W. W. Hager, “Updating the inverse of a matrix,” *SIAM Review. A Publication of the Society for Industrial and Applied Mathematics*, vol. 31, no. 2, pp. 221–239, 1989.
- [32] A. W. Marshall and I. Olkin, *Inequalities: Theory of Majorization and Its Applications*. Academic Press, 1979.
- [33] S. Ye and R. Blum, “Optimized signaling for MIMO interference systems with feedback,” *IEEE Transactions on Signal Processing*, vol. 51, no. 11, pp. 2839–2848, Nov. 2003.

APPENDIX I

PROOF OF THEOREM 1

We need to show that:

- 1) The action space of each player is convex and compact.
- 2) The utility function $U'_i(\tilde{\mathbf{T}}_i, \tilde{\mathbf{T}}_{-i})$ is concave with respect to (w.r.t) $\tilde{\mathbf{T}}_i$.

The action space of user i is shaped by constraints C1' and C2', which define the feasible region of the local optimization problem (10). It is easy to verify that the Hessians of C1' and C2' are positive definite. Hence, the two constraints are convex. Consequently, the feasible region or action space defined by constraints C1' and C2' are the intersection of two convex regions, i.e., the action space of the game (10) convex. Its compactness is due to the limit on the transmit power.

The utility function $U'_i(\tilde{\mathbf{T}}_i, \tilde{\mathbf{T}}_{-i})$ with the above price function can be written as:

$$\begin{aligned}
 U'_i(\tilde{\mathbf{T}}_i, \tilde{\mathbf{T}}_{-i}) &= \sum_{k \in \Psi_K} \log \det(\mathbf{I} + \tilde{\mathbf{T}}_i^{(k)H} \mathbf{H}_{d(i),i}^{(k)H} \mathbf{C}_{d(i)}^{(k)-1} \mathbf{H}_{d(i),i}^{(k)} \tilde{\mathbf{T}}_i^{(k)}) - \sum_{k \in \Psi_K} \text{tr} \left[\tilde{\mathbf{T}}_i^{(k)H} \mathbf{A}_i^{(k)} \tilde{\mathbf{T}}_i^{(k)} \right] \\
 &= \sum_{k \in \Psi_K} \{ \log \det(\mathbf{I} + \tilde{\mathbf{T}}_i^{(k)H} \mathbf{H}_{d(i),i}^{(k)H} \mathbf{C}_{d(i)}^{(k)-1} \mathbf{H}_{d(i),i}^{(k)} \tilde{\mathbf{T}}_i^{(k)}) - \text{tr} \left[\tilde{\mathbf{T}}_i^{(k)H} \mathbf{A}_i^{(k)} \tilde{\mathbf{T}}_i^{(k)} \right] \}.
 \end{aligned} \tag{29}$$

We observe that each frequency band f_k contributes its utility (and price) as the k th term in the expression of $U'_i(\tilde{\mathbf{T}}_i, \tilde{\mathbf{T}}_{-i})$. Using the positive-semidefiniteness assumption of $\mathbf{A}_i^{(k)}$ and the concavity of the link's rate, we can verify that each k th term of (29) is concave w.r.t $\tilde{\mathbf{T}}_i^{(k)}$, hence the overall utility function is concave w.r.t $\tilde{\mathbf{T}}_i$. Therefore, the game in (10) is a concave game, so it always admits at least one NE. \square

APPENDIX II

PROOF OF THEOREM 2

In Theorem 4, we prove that the game converges to a NE. We now need to show that the form of the pricing-factor matrix in (12) and (13) is the necessary and sufficient to ensure the achieved NE meets the K.K.T optimality conditions of (6). The achieved NE is characterized by the solutions of all N per-user optimization problems (10). For user i , the Lagrangian function is written as:

$$\begin{aligned}
& L_i(\tilde{\mathbf{T}}_i, \alpha_i^{(k)}, \gamma_i) \\
&= U'_i(\tilde{\mathbf{T}}_i, \tilde{\mathbf{T}}_{-i}) - \sum_{k \in \Psi_K} \alpha_i^{(k)} [\text{tr}(\tilde{\mathbf{T}}_i^{(k)} \tilde{\mathbf{T}}_i^{(k)H}) - P_{mask}(f_k)] - \gamma_i [\sum_{k \in \Psi_K} \text{tr}(\tilde{\mathbf{T}}_i^{(k)} \tilde{\mathbf{T}}_i^{(k)H}) - P_{\max}] \\
&= \sum_{k \in \Psi_K} \{R_i^{(k)} - \text{tr}(\tilde{\mathbf{T}}_i^{(k)H} \mathbf{A}_i^{(k)} \tilde{\mathbf{T}}_i^{(k)})\} - \sum_{k \in \Psi_K} \alpha_i^{(k)} [\text{tr}(\tilde{\mathbf{T}}_i^{(k)} \tilde{\mathbf{T}}_i^{(k)H}) - P_{mask}(f_k)] - \gamma_i [\sum_{k \in \Psi_K} \text{tr}(\tilde{\mathbf{T}}_i^{(k)} \tilde{\mathbf{T}}_i^{(k)H}) - P_{\max}]
\end{aligned} \tag{30}$$

where $\alpha_i^{(k)}$ and γ_i are the nonnegative Lagrangian multipliers. Since the individual utility optimization problem is convex, a locally optimal solution is thus globally optimal. The optimal solution can be found by solving its K.K.T. conditions [26], given by:

$$\begin{aligned}
\frac{\partial L_i(\tilde{\mathbf{T}}_i, \alpha_i^{(k)}, \gamma_i)}{\partial \tilde{\mathbf{T}}_i^{(k)*}} &= \frac{\partial R_i^{(k)}}{\partial \tilde{\mathbf{T}}_i^{(k)*}} - \mathbf{A}_i^{(k)} \tilde{\mathbf{T}}_i^{(k)} - (\alpha_i^{(k)} + \gamma_i) \tilde{\mathbf{T}}_i^{(k)} = 0, \forall k \in \Psi_K \\
\sum_{k \in \Psi_K} \text{tr}(\tilde{\mathbf{T}}_i^{(k)} \tilde{\mathbf{T}}_i^{(k)H}) - P_{\max} &\leq 0 \\
\gamma_i [\sum_{k \in \Psi_K} \text{tr}(\tilde{\mathbf{T}}_i^{(k)} \tilde{\mathbf{T}}_i^{(k)H}) - P_{\max}] &= 0 \\
\text{tr}(\tilde{\mathbf{T}}_i^{(k)} \tilde{\mathbf{T}}_i^{(k)H}) - P_{mask}(f_k) &\leq 0, \forall k \in \Psi_K \\
\alpha_i^{(k)} [\text{tr}(\tilde{\mathbf{T}}_i^{(k)} \tilde{\mathbf{T}}_i^{(k)H}) - P_{mask}] &= 0, \forall k \in \Psi_K
\end{aligned} \tag{31}$$

The Lagrangian function of the network optimization problem (6) is:

$$\begin{aligned}
& L(\tilde{\mathbf{T}}, \alpha_i^{(k)}, \gamma_i) \\
&= \sum_{i \in \Phi_N} R_{(i)} - \sum_{i \in \Phi_N} \sum_{k \in \Psi_K} \alpha_i^{(k)} [\text{tr}(\tilde{\mathbf{T}}_i^{(k)} \tilde{\mathbf{T}}_i^{(k)H}) - P_{mask}(f_k)] - \sum_{i \in \Phi_N} \gamma_i \left[\sum_{k \in \Psi_K} \text{tr}(\tilde{\mathbf{T}}_i^{(k)} \tilde{\mathbf{T}}_i^{(k)H}) - P_{\max} \right] \\
&= \sum_{i \in \Phi_N} \sum_{k \in \Psi_K} R_i^{(k)} - \sum_{i \in \Phi_N} \sum_{k \in \Psi_K} \alpha_i^{(k)} [\text{tr}(\tilde{\mathbf{T}}_i^{(k)} \tilde{\mathbf{T}}_i^{(k)H}) - P_{mask}(f_k)] - \sum_{i \in \Phi_N} \gamma_i \left[\sum_{k \in \Psi_K} \text{tr}(\tilde{\mathbf{T}}_i^{(k)} \tilde{\mathbf{T}}_i^{(k)H}) - P_{\max} \right]
\end{aligned} \tag{32}$$

where $\tilde{\mathbf{T}} \stackrel{\text{def}}{=} \bigcup_i \tilde{\mathbf{T}}_i$ is the set of precoding matrices over all users and frequency bands.

All of the stationary or locally optimal points of the network problem must satisfy the its K.K.T. conditions:

$$\begin{aligned}
\frac{\partial L(\tilde{\mathbf{T}}, \alpha_i^{(k)}, \gamma_i)}{\partial \tilde{\mathbf{T}}_i^{(k)*}} &= \frac{\partial R_i^{(k)}}{\partial \tilde{\mathbf{T}}_i^{(k)*}} + \sum_{j \in \Phi_N \setminus \{i\}} \frac{\partial R_j^{(k)}}{\partial \tilde{\mathbf{T}}_i^{(k)*}} - (\alpha_i^{(k)} + \gamma_i) \tilde{\mathbf{T}}_i^{(k)} = 0, \forall k \in \Psi_K, \forall i \in \Phi_N \\
& \sum_{k \in \Psi_K} \text{tr}(\tilde{\mathbf{T}}_i^{(k)} \tilde{\mathbf{T}}_i^{(k)H}) - P_{\max} \leq 0, \forall i \in \Phi_N \\
\gamma_i \left[\sum_{k \in \Psi_K} \text{tr}(\tilde{\mathbf{T}}_i^{(k)} \tilde{\mathbf{T}}_i^{(k)H}) - P_{\max} \right] &= 0, \forall i \in \Phi_N \\
\text{tr}(\tilde{\mathbf{T}}_i^{(k)} \tilde{\mathbf{T}}_i^{(k)H}) - P_{mask}(f_k) &\leq 0, \forall k \in \Psi_K, \forall i \in \Phi_N \\
\alpha_i^{(k)} [\text{tr}(\tilde{\mathbf{T}}_i^{(k)} \tilde{\mathbf{T}}_i^{(k)H}) - P_{mask}] &= 0, \forall k \in \Psi_K, \forall i \in \Phi_N
\end{aligned} \tag{33}$$

To guarantee that the game (10) with the price function defined in (11) converges to a NE at which the CRN's throughput is the same as that of a locally optimal solution to problem (6), the NE of the game (10) must be a stationary point of problem (6). In other words, the K.K.T. conditions of (6) have to hold at the stationary point of (10). For that to happen, the following equality must hold (by comparing (31) and (33)):

$$-\mathbf{A}_i^{(k)} \tilde{\mathbf{T}}_i^{(k)} = \sum_{j \in \Phi_N \setminus \{i\}} \frac{\partial R_j^{(k)}}{\partial \tilde{\mathbf{T}}_i^{(k)*}}. \tag{34}$$

To compute $\frac{\partial R_j^{(k)}}{\partial \tilde{\mathbf{T}}_i^{(k)*}}$, recall (2) and note that:

$$R_j^{(k)} = \log \det(\mathbf{C}_{d(j)}^{(k)} + \mathbf{H}_{d(j),j}^{(k)} \tilde{\mathbf{T}}_j^{(k)} \tilde{\mathbf{T}}_j^{(k)H} \mathbf{H}_{d(j),j}^{(k)H}) - \log \det(\mathbf{C}_{d(j)}^{(k)})$$

and

$$\mathbf{C}_{d(j)}^{(k)} = \mathbf{I} + \mathbf{H}_{d(j),i}^{(k)} \tilde{\mathbf{T}}_i^{(k)} \tilde{\mathbf{T}}_i^{(k)H} \mathbf{H}_{d(j),i}^{(k)H} + \sum_{v \in \Phi_N \setminus \{i,j\}} \mathbf{H}_{d(j),v}^{(k)} \tilde{\mathbf{T}}_v^{(k)} \tilde{\mathbf{T}}_v^{(k)H} \mathbf{H}_{d(j),v}^{(k)H}.$$

We have

$$\begin{aligned} \frac{\partial R_j^{(k)}}{\partial \tilde{\mathbf{T}}_i^{(k)*}} &= -\mathbf{H}_{d(j),i}^{(k)H} \mathbf{C}_{d(j)}^{(k)-1} \mathbf{H}_{d(j),i}^{(k)} \tilde{\mathbf{T}}_i^{(k)} + \mathbf{H}_{d(j),i}^{(k)H} (\mathbf{C}_{d(j)}^{(k)} + \mathbf{H}_{d(j),j}^{(k)} \tilde{\mathbf{T}}_j^{(k)} \tilde{\mathbf{T}}_j^{(k)H} \mathbf{H}_{d(j),j}^{(k)H})^{-1} \mathbf{H}_{d(j),i}^{(k)} \tilde{\mathbf{T}}_i^{(k)} \\ &= -\mathbf{H}_{d(j),i}^{(k)H} \mathbf{C}_{d(j)}^{(k)-1} \mathbf{H}_{d(j),j}^{(k)} [(\tilde{\mathbf{T}}_j^{(k)} \tilde{\mathbf{T}}_j^{(k)H})^{-1} + \mathbf{H}_{d(j),j}^{(k)H} \mathbf{C}_{d(j)}^{(k)-1} \mathbf{H}_{d(j),j}^{(k)}]^{-1} \mathbf{H}_{d(j),j}^{(k)H} \mathbf{C}_{d(j)}^{(k)-1} \mathbf{H}_{d(j),i}^{(k)} \tilde{\mathbf{T}}_i^{(k)}. \end{aligned} \quad (35)$$

The last equality in (35) follows by applying the Woodbury identity [31] to $(\mathbf{C}_{d(j)}^{(k)} + \mathbf{H}_{d(j),j}^{(k)} \tilde{\mathbf{T}}_j^{(k)} \tilde{\mathbf{T}}_j^{(k)H} \mathbf{H}_{d(j),j}^{(k)H})^{-1}$. Plugging (35) into (34), we get (13). One can also easily verify that the derived $\mathbf{A}_i^{(k)}$ matrix is positive-semidefinite. Additionally, if the pricing-factor has the form (13), the achieved NE meets the K.K.T conditions of the problem (6) (sufficient condition). \square

APPENDIX III

PROOF OF THEOREM 3

Let's rewrite the Lagrangian function of (10) as follows:

$$\begin{aligned} L_i(\tilde{\mathbf{T}}_i, \alpha_i^{(k)}, \gamma_i) &= \sum_{k \in \Psi_K} \{ \log \det(\mathbf{I} + \tilde{\mathbf{T}}_i^{(k)H} \mathbf{H}_{d(i),i}^{(k)H} \mathbf{C}_{d(i)}^{(k)-1} \mathbf{H}_{d(i),i}^{(k)} \tilde{\mathbf{T}}_i^{(k)}) \\ &\quad - \text{tr}(\tilde{\mathbf{T}}_i^{(k)H} \mathbf{A}_i^{(k)} \tilde{\mathbf{T}}_i^{(k)}) - \alpha_i^{(k)} \text{tr}(\tilde{\mathbf{T}}_i^{(k)} \tilde{\mathbf{T}}_i^{(k)H}) \\ &\quad - \gamma_i \text{tr}(\tilde{\mathbf{T}}_i^{(k)} \tilde{\mathbf{T}}_i^{(k)H}) + \alpha_i^{(k)} P_{mask}(f_k) + \frac{\gamma_i}{K} P_{\max} \} \\ &= \sum_{k \in \Psi_K} \{ \log \det(\mathbf{I} + \tilde{\mathbf{T}}_i^{(k)H} \mathbf{H}_{d(i),i}^{(k)H} \mathbf{C}_{d(i)}^{(k)-1} \mathbf{H}_{d(i),i}^{(k)} \tilde{\mathbf{T}}_i^{(k)}) \\ &\quad - \text{tr}(\tilde{\mathbf{T}}_i^{(k)H} [\mathbf{A}_i^{(k)} + (\alpha_i^{(k)} + \gamma_i) \mathbf{I}] \tilde{\mathbf{T}}_i^{(k)}) \\ &\quad + \alpha_i^{(k)} P_{mask}(f_k) + \frac{\gamma_i}{K} P_{\max} \}. \end{aligned} \quad (36)$$

Using the following Cholesky decomposition

$$[\mathbf{A}_i^{(k)} + (\alpha_i^{(k)} + \gamma_i) \mathbf{I}] = \mathbf{E}_i^{(k)} \mathbf{E}_i^{(k)H} \quad (37)$$

We have

$$\begin{aligned}
L_i(\tilde{\mathbf{T}}_i, \alpha_i^{(k)}, \gamma_i) &= \sum_{k \in \Psi_K} \{ \log \det(\mathbf{I} + \tilde{\mathbf{T}}_i^{(k)H} \mathbf{H}_{d(i),i}^{(k)H} \mathbf{C}_{d(i)}^{(k)-1} \mathbf{H}_{d(i),i}^{(k)} \tilde{\mathbf{T}}_i^{(k)}) \\
&\quad - \text{tr}(\tilde{\mathbf{T}}_i^{(k)H} \mathbf{E}_i^{(k)} \tilde{\mathbf{T}}_i^{(k)}) + \alpha_i^{(k)} P_{mask}(f_k) + \frac{\gamma_i}{K} P_{\max} \} \\
&= \sum_{k \in \Psi_K} \{ \alpha_i^{(k)} P_{mask}(f_k) + \frac{\gamma_i}{K} P_{\max} - \text{tr}(\bar{\mathbf{T}}_i^{(k)H} \bar{\mathbf{T}}_i^{(k)}) \\
&\quad + \log \det(\mathbf{I} + \bar{\mathbf{T}}_i^{(k)H} \mathbf{E}_i^{(k)-1} \mathbf{H}_{d(i),i}^{(k)H} \mathbf{C}_{d(i)}^{(k)-1} \mathbf{H}_{d(i),i}^{(k)} \mathbf{E}_i^{(k)H-1} \bar{\mathbf{T}}_i^{(k)}) \}
\end{aligned} \tag{38}$$

where $\bar{\mathbf{T}}_i^{(k)H} = \tilde{\mathbf{T}}_i^{(k)H} \mathbf{E}_i^{(k)}$.

We now follow the routine of using Hadamard inequality (e.g., [14], [12]). As P_{\max} and $P_{mask}(f_k)$ are predetermined values and from (38), L_i is maximized if we maximize

$$L'_i = \sum_{k \in \Psi_K} \{ -\text{tr}(\bar{\mathbf{T}}_i^{(k)H} \bar{\mathbf{T}}_i^{(k)}) + \log \det(\mathbf{I} + \bar{\mathbf{T}}_i^{(k)H} \mathbf{E}_i^{(k)-1} \mathbf{H}_{d(i),i}^{(k)H} \mathbf{C}_{d(i)}^{(k)-1} \mathbf{H}_{d(i),i}^{(k)} \mathbf{E}_i^{(k)H-1} \bar{\mathbf{T}}_i^{(k)}) \} \tag{39}$$

Applying the Hadamard's inequality [32] to the second term of (39), we have:

$$L'_i \leq \sum_{k \in \Psi_K} \{ -\text{tr}(\bar{\mathbf{T}}_i^{(k)H} \bar{\mathbf{T}}_i^{(k)}) + \sum_{s=1}^M \log(1 + \text{diag}_s \{ \bar{\mathbf{T}}_i^{(k)H} \mathbf{E}_i^{(k)-1} \mathbf{H}_{d(i),i}^{(k)H} \mathbf{C}_{d(i)}^{(k)-1} \mathbf{H}_{d(i),i}^{(k)} \mathbf{E}_i^{(k)H-1} \bar{\mathbf{T}}_i^{(k)} \}) \} \tag{40}$$

where $\text{diag}_s(\cdot)$ is the (s, s) diagonal element of a matrix (\cdot) .

The equality happens when $\bar{\mathbf{T}}_i^{(k)H} \mathbf{E}_i^{(k)-1} \mathbf{H}_{d(i),i}^{(k)H} \mathbf{C}_{d(i)}^{(k)-1} \mathbf{H}_{d(i),i}^{(k)} \mathbf{E}_i^{(k)H-1} \bar{\mathbf{T}}_i^{(k)}$ is a diagonal matrix. This is the case if there exists an orthonormal matrix $\bar{\mathbf{T}}_i^{(k)}$ that diagonalizes the matrix $\mathbf{E}_i^{(k)-1} \mathbf{H}_{d(i),i}^{(k)H} \mathbf{C}_{d(i)}^{(k)-1} \mathbf{H}_{d(i),i}^{(k)} \mathbf{E}_i^{(k)H-1}$.

Hence, we should have $\bar{\mathbf{T}}_i^{(k)H} \bar{\mathbf{T}}_i^{(k)} = \mathbf{I}$ and

$$\bar{\mathbf{T}}_i^{(k)-1} \mathbf{E}_i^{(k)-1} \mathbf{H}_{d(i),i}^{(k)H} \mathbf{C}_{d(i)}^{(k)-1} \mathbf{H}_{d(i),i}^{(k)} \mathbf{E}_i^{(k)H-1} \bar{\mathbf{T}}_i^{(k)} = \mathbf{\Lambda}_i^{(k)} \tag{41}$$

where $\mathbf{\Lambda}_i^{(k)}$ is a $M \times M$ diagonal matrix.

Multiply both sides of (41) by $\bar{\mathbf{T}}_i^{(k)}$, then $\mathbf{E}_i^{(k)}$, we have:

$$\mathbf{H}_{d(i),i}^{(k)H} \mathbf{C}_{d(i)}^{(k)-1} \mathbf{H}_{d(i),i}^{(k)} \mathbf{E}_i^{(k)H-1} \bar{\mathbf{T}}_i^{(k)} = \mathbf{E}_i^{(k)} \bar{\mathbf{T}}_i^{(k)} \mathbf{\Lambda}_i^{(k)}.$$

Recall that $\bar{\mathbf{T}}_i^{(k)H} = \tilde{\mathbf{T}}_i^{(k)H} \mathbf{E}_i^{(k)}$. Using the Cholesky decomposition in (37), we have:

$$\mathbf{H}_{d(i),i}^{(k)H} \mathbf{C}_{d(i)}^{(k)-1} \mathbf{H}_{d(i),i}^{(k)} \tilde{\mathbf{T}}_i^{(k)} = \mathbf{E}_i^{(k)} \mathbf{E}_i^{(k)H} \tilde{\mathbf{T}}_i^{(k)} \boldsymbol{\Lambda}_i^{(k)} = [\mathbf{A}_i^{(k)} + (\alpha_i^{(k)} + \gamma_i) \mathbf{I}] \tilde{\mathbf{T}}_i^{(k)} \boldsymbol{\Lambda}_i^{(k)}.$$

This concludes the proof. □

APPENDIX IV

PROOF OF THEOREM 4

To establish the convergence of the distributed algorithm, one can find a Lyapunov-type function of the precoding matrices and show that the function is non-decreasing and upper-bounded e.g., [9]. Let's define such a function as the total network throughput.

$$\begin{aligned} F(\tilde{\mathbf{T}}) &= \sum_{i \in \Phi_N} U_i(\tilde{\mathbf{T}}_i, \tilde{\mathbf{T}}_{-i}) \\ &= U_i(\tilde{\mathbf{T}}_i, \tilde{\mathbf{T}}_{-i}) + \sum_{j \in \{\Phi_N \setminus \{i\}\}} U_j(\tilde{\mathbf{T}}_j, \tilde{\mathbf{T}}_{-j}) \\ &= U'_i(\tilde{\mathbf{T}}_i, \tilde{\mathbf{T}}_{-i}) + \sum_{k \in \Psi_K} \{\text{tr}(\tilde{\mathbf{T}}_i^{(k)H} \mathbf{A}_i^{(k)} \tilde{\mathbf{T}}_i^{(k)}) + R_{-i}^{(k)}(\tilde{\mathbf{T}}_j, \tilde{\mathbf{T}}_{-j})\} \end{aligned} \tag{42}$$

where $R_{-i}^{(k)}(\tilde{\mathbf{T}}_j, \tilde{\mathbf{T}}_{-j}) \stackrel{\text{def}}{=} \sum_{j \in \{\Phi_N \setminus \{i\}\}} R_j^{(k)}(\tilde{\mathbf{T}}_j, \tilde{\mathbf{T}}_{-j})$ is the total throughput from all users except user i on frequency band k .

During the training window, a node can use either Gauss-Seidel (sequential) or Jacobi (parallel) iteration methods to update its precoding matrices. If using sequential updating mechanism, at the iteration step $(t + 1)$ of user i : $\tilde{\mathbf{T}} = \tilde{\mathbf{T}}(t + 1) \stackrel{\text{def}}{=} \tilde{\mathbf{T}}_i(t + 1) \cup \tilde{\mathbf{T}}_{-i}(t)$.

We have:

$$\begin{aligned}
& F(\tilde{\mathbf{T}}(t+1)) \\
&= U'_i(\tilde{\mathbf{T}}(t+1)) + \sum_{k \in \Psi_K} \{\text{tr}(\tilde{\mathbf{T}}_i^{(k)H}(t+1)\mathbf{A}_i^{(k)}\tilde{\mathbf{T}}_i^{(k)}(t+1)) + R_{-i}^{(k)}(\tilde{\mathbf{T}}(t+1))\} \\
&\geq U'_i(\tilde{\mathbf{T}}(t)) + \sum_{k \in \Psi_K} \{\text{tr}(\tilde{\mathbf{T}}_i^{(k)H}(t+1)\mathbf{A}_i^{(k)}\tilde{\mathbf{T}}_i^{(k)}(t+1)) + R_{-i}^{(k)}(\tilde{\mathbf{T}}(t+1))\} \\
&= U_i(\tilde{\mathbf{T}}(t)) + \sum_{k \in \Psi_K} R_{-i}^{(k)}(\tilde{\mathbf{T}}(t)) + \sum_{k \in \Psi_K} \{\text{tr}((\tilde{\mathbf{T}}_i^{(k)}(t+1) - \tilde{\mathbf{T}}_i^{(k)}(t)) \frac{\partial R_{-i}^{(k)}(\tilde{\mathbf{T}})}{\partial \tilde{\mathbf{T}}_i^{(k)}}) + (R_{-i}^{(k)}(\tilde{\mathbf{T}}(t+1)) - R_{-i}^{(k)}(\tilde{\mathbf{T}}(t)))\} \\
&= \sum_{i \in \Phi_N} U_i(\tilde{\mathbf{T}}(t)) + \sum_{k \in \Psi_K} \text{tr}\{(\tilde{\mathbf{T}}_i^{(k)}(t+1) - \tilde{\mathbf{T}}_i^{(k)}(t)) \frac{\partial R_{-i}^{(k)}(\tilde{\mathbf{T}})}{\partial \tilde{\mathbf{T}}_i^{(k)}} + (R_{-i}^{(k)}(\tilde{\mathbf{T}}(t+1)) - R_{-i}^{(k)}(\tilde{\mathbf{T}}(t)))\}.
\end{aligned} \tag{43}$$

In the above, we have used the expression of $\mathbf{A}_i^{(k)}$ in (34) and the fact that $\tilde{\mathbf{T}}_i(t+1)$ is the new optimal solution of link i . To prove that the second summation in the last equality of (43) is nonnegative, we now can follow a similar method used in [33] and [14] by verifying the convexity of $R_{-i}^{(k)}(\tilde{\mathbf{T}})$ w.r.t to $\tilde{\mathbf{T}}_i^{(k)}$ (checking the positive definiteness of its Hessian). Consequently, the total network throughput is a non-decreasing function of the the latest precoding matrices at user i (simulations confirm it in Figure 4)

$$F(\tilde{\mathbf{T}}(t+1)) \geq F(\tilde{\mathbf{T}}(t))$$

The upper-bound of total network throughput $F(\tilde{\mathbf{T}})$ is easily to be shown under the power limitation and perfect interference cancelation (or interference-free) assumption. Therefore, the distributed algorithm under sequential updating procedure must converge. The converged point must be a NE, otherwise one user can still unilaterally improves its return $U'_i(\tilde{\mathbf{T}}_i, \tilde{\mathbf{T}}_{-i})$ (that violates the convexity of the individual problem (10)). \square